AFML-TR-67-423

EFFECTS OF ENVIRONMENTAL FACTORS ON COMPOSITE MATERIALS

J. C. HALPIN

TECHNICAL REPORT AFML-TR-67-423

JUNE 1969

AIR FORCE MATERIALS LABORATORY
AIR FORCE SYSTEMS COMMAND
WRIGHT-PATTERSON AIR FORCE BASE, OHIO 45433

AFML-TR-67-423

EFFECTS OF ENVIRONMENTAL FACTORS ON COMPOSITE MATERIALS

J. C. HALPIN

FOREWORD

This report was prepared by J. C. Halpin of the Elastomers and Coatings Branch, Nonmetallic Materials Division, Air Force Materials Laboratory. The work was conducted under Project No. 7342, "Fundamental Research on Macromolecular Materials and Lubrication Phenomena," Task No. 734202, "Studies on the Structure-Property Relationships of Polymeric Materials," and was administered by the Air Force Materials Laboratory, Air Force Systems Command, Wright-Patterson Air Force Base, Ohio.

This report covers research conducted from August 1967 to December 1967. This report was released by the author in October 1968.

This technical report has been reviewed and is approved.

W. P. Johnson, Chief
Elastomers and Coatings Branch
Nonmetallic Materials Division
Air Force Materials Laboratory

ABSTRACT

Some of the environmental factors which affect the structural performance of composite materials are discussed. Various possible mechanisms of environmental factors are examined, together with relevant experimental data. Finally, an analytical approach for predicting environmental effects, based on rate theory, is considered.

TABLE OF CONTENTS

ILLUSTRATIONS

ILLUSTRATIONS (CONTD)

SECTION I

INTRODUCTION

The superior strength and stiffness of composite materials are often compromised in their structural usage by the uncertainty of the material behavior under cyclic and impact loading and various environmental factors, e.g., exposure to water, water vapor or other corrosive environments, change in temperature, and long-term physical and chemical stability. Since reliable theory and experimental data are practically nonexistent, superior properties of composite materials are severely penalized by the use of unusually large margins of safety in actual design. Thus, the immediate future of composite materials as a class of engineering materials may depend more on improved reliability of present-day composites than on the production of new composites. Universal acceptance of composites as high performance materials will depend very much on the confidence of the designer and user of the materials. Until the degradation of composite materials by various environmental factors is better understood so that corrective measures can be taken, the true potential of such materials cannot be realized.

The apparent causes of degradation may involve several factors:

1. Loss of strength of the reinforcing fibers by a stress-corrosion mechanism.

2. Degradation of the fiber-matrix interface resulting in loss of adhesion and interfacial bond strength.

3. Permeability of the matrix material to corrosive agents, such as water vapor, which affects both 1 and 2 above.

4. Normal viscoelastic dependence of matrix modulus and strength on time and temperature.

5. Accelerated degradation from the combined action of temperature and moisture. As a result of these environmental factors, the utility of composite materials is terminated when the stiffness is reduced sufficiently to cause structural instability, and/or failure or rupture of the material is induced.

SECTION II

MATHEMATICAL FRAMEWORK

Before each of the environmental factors is examined in detail, it may be useful to define a general framework through which the relevance of the environmental factors to the structural performance of composite materials can be properly established. One important characteristic of composite materials is their macroscopic anisotropy. The properties measured in the longitudinal direction of a unidirectional composite are, in general, quite different from those in the transverse direction. Any attempt at understanding the effect of environmental factors must take into account the inherent anisotropy of the composite. One theory which has been found experimentally to yield reasonably accurate strength prediction is Hill's criterion for orthotropic materials (References 1 and 2). For two-dimensional orthotropic bodies, this theory states that the strength depends on three principal strengths, viz., the longitudinal, transverse, and shear strengths. Degradation of the principal strengths by a given environmental factor will not be to the same degree, e.g., stress corrosion of fibers will probably degrade the longitudinal strength more than the transverse and shear strengths on a percentage basis, and "plasticization" of the matrix will probably affect the transverse and shear strengths more than the longitudinal strength. Thus, a crucial question from a designer's viewpoint is how to assess the environmental factors on the total performance of the composite materials, which, in the most common configuration are in the form of laminated anisotropic bodies. A large reduction of the longitudinal strength alone may or may not have significance effects on the total performance of the composite. This points toward the need of a mathematical framework into which theoretical and experimental efforts can be properly integrated. A great deal of existing work on the environmental effects has been concerned with segmented problem areas, and it is difficult to assess their relevance to the total performance of composites.

Although current mechanics theory of composites has not provided a reasonably realistic yet tractable mathematical model of the general process of degradation, the need for a consistent framework should be fully appreciated.

The elastic properties of composite materials can be conveniently divided into micro and macromechanics. Micromechanics study takes into account the local heterogeneity, which reduces the study to the problem of multiple isotropic inclusions, whereas macromechanics study is concerned with quasi-homogeneous anisotropic layered media. The bridge between micro and macromechanics is the unidirectional layer.

A similar approach of micro and macromechanics for the study of environmental factors should be adopted. Basically, the behavior of a unidirectional composite is orthotropic and can thus be described by four principal elastic constants and three principal strengths. The number of the elastic constants is exact in the mathematical sense but that of the principal strengths is only approximate and depends on the theory used. It should be fruitful to describe the environmental interaction in terms of the degradation of the orthotropic elastic constants and strengths.

SECTION III

FIBER STRENGTH

In principle, the strength of materials is limited by the magnitude of the forces that bind atoms together. In practice, the "strength" of most solids is determined or limited by imperfections or flaws. In glasses and other amorphous solids, the important imperfections are surface cracks or other flaws that grow under the influence of stress and chemical attack. It is common experimental knowledge that, when subjected to appropriate environments, many hard amorphous or crystalline solids exhibit a type of failure in which the strength is markedly influenced by the time during which the load is applied. For example, it is a known fact that humid atmospheres reduce the breaking strength of silicate glasses, and that the strength of many plastics is impaired when immersed in detergent solutions and solvents.

Since breaking stresses are generally small in comparison with the theoretical limits, the failure phenomena must include reference to defects or flaws, and since failure is time dependent, it is natural to conclude that the defects are subject to change during the test. For example, the strength of silicate glasses is notably sensitive to abrasion, and it is generally accepted that surface flaws are controlling influences. Most workers have found it logical to assume that delayed failure under constant load is caused by the growth of these flaws, under the influence of a reactive environment, to a critical size at which the stress concentration at the most critical flaw is sufficient for spontaneous failure. The occurrence of fracture depends, therefore, on the state of the material. If there is a flaw of sufficient dimensions, which depends on the state of stress and the bulk properties of the material, prompt fracture is certain; and if there is no such flaw, the sample is sure to survive until a flaw qualifies through flaw growth, stress increase, or time dependent changes in bulk properties.

In general, details of stress corrosion mechanisms for different materials and environments are not well understood. However, all systems have similar

attributes or consequences:

1. In inert environments or at low temperatures, where the reaction rate of corrosion processes should be negligibly slow, the breaking strengths of materials become independent of the duration of load and always reach a relatively high value.

2. Equivalently high strengths are observed if the loading rate is rapid with respect to the reaction rate.

3. Exposing these materials to reactive environments before, but not during a test generally has little effect on test results, suggesting that the corrosion rate is accelerated by the stress.

4. Exposure of these materials to reactive environments during a test leads to delayed rupture at strengths substantially reduced with respect to comments 1 and 3 above.

5. There is a continuous influence of temperature on the relationship between the time of loading and the failure stress. In general, a continuous loss of strength occurs with increasing temperatures.

Thus, the usage of brittle high strength fibrous materials is limited by a time dependent distribution of flaw sizes. If only strength degradation of fibers occurs in a fibrous composite, the longitudinal strength of a unidirectional composite will be seriously affected, but there will be only a slight alternation of the transverse and shear strengths.

It is not suprising to discover that the coating of fibers or their incorporation into a matrix provides a means of exploiting the properties of these high strength reinforcement materials, for the coating or "coupling agent" acts to protect the fibers from abrasion or other sources of surface flaws during fabrication as well as providing, along with the matrix, a barrier between the aggressive environment and the reinforcement. High strength reinforcements are also developed with specific efforts devoted to achieving a chemical composition which is inert with respect to the anticipated service environment.

Extensive data on the effect of water or water vapor on glass-reinforced composites are available and will not be covered here. Typical results for a

glass-epoxy composite have been reported by Boller (Reference 3) and are shown in Figure 1. In these experiments the unidirectional composites were under a constant uniaxial stress at constant temperatures in a water environment as indicated in Figure 1. We found that relative humidity and water immersion experiments lead to a continuous loss of strength with increasing time, the rate of strength loss being greatly accelerated by the immersion experiments. It is tempting to suggest that the total immersion curve represents the extremely long time asymptote for the humid aging environment characterizing the interaction between water-silica glass, time, and stress. However, such a simple correlation must be tempered with the knowledge that excessive absorption of water in the matrix induces a mechanical damage to the matrix which may or may not be realized in long term exposures to outer atmospheres containing reduced concentrations of water vapor. This point is discussed in more detail in a later section.

Results of water-boil tests of boron-epoxy (Narmco 5505) composites were reported by General Dynamics/Fort Worth Division (Reference 4). After boiling in tap water for two hours, the longitudinal strength of the unidirectional composite was degraded by a maximum of 6%. Presumably, degradation of longitudinal strength of boron-epoxy composites in humid atmospheres will be substantially less than glass-epoxy systems; however, further data are needed.,

Qualitative information regarding the importance of the stress-corrosion process can be obtained through measurements of the time dependent longitudinal strength and stiffness, but other factors also influence the test data so that it is rather difficult to obtain quantitative information. Detailed investigations will require the examination of relationships of relative humidity or water concentration in the composite with the "time to rupture" at a particular value of the stress, and how the experimental variables change with a change in temperature. It is an obvious experimental fact that the failure of these systems is strongly influenced by a time-dependent stress-corrosion phenomenon.

SECTION IV

INTERFACE

Degradation of composite properties due to environmental effects may be attributed to the loss of adhesion and bond strength at the fiber-matrix interface. It has been shown that the passage of water along the interface is at a rate much higher than permeation through the matrix in a glass-epoxy laminate. If passage of water destroys the interfacial bond, this would result in some form of degradation in the composite properties. Studies of interfacial bonds are rather crude at the present time but we do have some qualitative information: a) the addition of coupling agents promoting adhesion between phases results in a slight increase in longitudinal stiffness and strength when tested in the dry state; and b) when tested under wet conditions the untreated fibrous composites posses low strength which increases strongly with coating agent concentration until the "dry" strength is approached.

Failure of the interface bond is termed dewetting. Although this phenomenon has been observed for some time in the study of reinforced elastomers and solid rocket motors, it cannot be predicted analytically with any reliability. The "interfacial strength" may be easier to determine experimentally from the transverse and shear properties of a unidirectional composite than the longitudinal properties. Again, the intrusion of "environmental" factors will greatly affect the analysis because the variability of the interface properties will depend upon the time scale of observation.

SECTION V
MATRIX EFFECTS

A. IRREVERSIBLE TEMPERATURE EFFECTS

In many instances of military engineering interest, composite systems will be exposed to excessive temperatures for varying periods of time. In general, organic matrix materials are unstable with respect to increased temperature and undergo a chemical breakdown which we shall denote as thermal degradation. If the degradation reactions persist for a sufficient length of time or if they are sufficiently rapid, then there will occur enough chemical degradation to cause the matrix material to vaporize. Of course such drastic events compromise the mechanical integrity of the composite system and provide an upper bound on temperature in materials technology. One semiquantitative procedure to follow and characterize the degradation process is the measure of the amount of volatiles given off by the material as a function of time and temperature or simply to record the weight loss as a function of time and temperature. Such data (Reference 3) are shown in Figure 2 for a phenolic-glass system. At all temperatures of 300° F and above, decomposition of the matrix is occurring at a "rate" which is uniformly accelerated with increasing temperature. If the weight loss curves are shifted relative to each other along the log t axis, the curves overlap so as to form a single smooth curve, Figure 3. The shift distances along the log time scale are denoted by the symbolism log a_D. In Figure 3, the data was shifted (Reference 5) to the 300° F curve and one can readily see that the data obtained at different temperatures defines a composite curve representative of the decomposition process. Hence, it appears that a time-temperature superposition applies to this type of data.

It is expected that a temperature-time superposition will be valid in any rate process for which the temperature influences only the rate constant k. In such a case the process under consideration will be a function of the product kt, where t is the time for which the process has been going on. Even when the temperature enters the mathematical function describing the behavior in a more complicated way than this, it is still usually true that the major temperature dependence is through the rate constant. If k_o is called the rate constant at the

at the reference temperature (i.e., the temperature for the data to which the other data are shifted; in our case, 300°F) and k the rate constant at any other temperature, then log (k/k_o) is the amount by which the data must be shifted along the log t axis, our log a_D. The values of log a_D or log (k/k_o) are often plotted against reciprocal temperature with the following interpretation.

If the rate constant takes the form

$$k = A \exp(-\Delta H/RT) \tag{1}$$

then the ratio of the change in rate constants for temperatures T and T_o is written

$$\log (k/k_o) = \log a_D = -\frac{\Delta H}{2.303R}\left(\frac{1}{T} - \frac{1}{T_o}\right) \tag{2}$$

where ΔH is the activation energy and R is the gas constant. Thus, a plot of log a_D against 1/T should give rise to a straight line of slope $\Delta H/2.303R$. In Figure 4 a plot of this nature has been constructed (Reference 5) from the data of Figure 3, from which an apparent activation energy of 7.85 K cal/mole was computed. This activation energy is considered to be of the proper order of magnitude for the process involved.

Returning to Figure 3 we see that the experimental data can be approximated by either

$$\frac{w(t) - w(\infty)}{w(o) - w(\infty)} = 1 - \exp(-kt)$$

or (3)

$$\frac{w(t) - w(\infty)}{w(o) - w(\infty)} = 1 - \exp(-kt^2)$$

where w (t) is percent weight loss at time t, w (∞) at infinite time, in this case 3%, and w (o) is condition at t = o, or zero. Figure 3 clearly shows that exposure of this phenolic-glass composite to 300° F for times in excess of values between 5.0×10^3 and 10^4 hours leads to a significant change in matrix properties through thermal decomposition. If one now wishes to estimate the extent of degradation at 500° F, one simply shifts the entire master curve of Figure 3 to the left by two decades and so on.

Now, if matrix decomposition occurs, this must ultimately lead to a loss in stiffness and strength which would parallel the loss of the matrix integrity. In fact, Boller has obtained data in tension, compression, and flexure for the phenolic-glass composite samples which were soaked at the same temperatures presented in Figure 2 for different periods of time. The data generally shows the same trends as those presented in Figure 2. If there is a deterministic relationship between matrix decomposition and mechanical response, then the data can be shifted by the same log a_D values evaluated in Figure 4 to obtain master curves of stiffness and strength loss. The results are shown in Figure 5, where one can also see that the mechanical property loss is following the same rate law, $\exp(-kt^2)$, as the decomposition reaction. Also illustrated in Figure 5 is the proportionality between the loss of modulus and the parallel loss in strength or

$$\sigma(t) \simeq 0.01\, E(t) \tag{4}$$

Thus it appears that ultimately rather simple deterministic relations between thermal stability and matrix modulus to predict composite stiffness can be developed, and in turn, a cause-effect relationship between the time-temperature dependent stiffness and the "strength" of the composite. Hopefully, then there would evolve a continuous theory going from the physical chemistry of composite materials to the mechanical response of a structural unit.

We may further reinforce the ideas presented here by considering some data obtained by Stevens (Reference 6) in fatigue experiments conducted at different temperatures. Figure 6 represents experimental results for a phenolic-glass composite. These results are typical for this type of experiment. An increase in temperature clearly accelerates the rate of fatigue damage imparted at a given stress level. For example, a maximum stress of 20,000 psi gives instantaneous rupture at 800° F, rupture after 250 cycles at 500° F, after 1.78×10^4 cycles at 300° F, and 2.0×10^5 cycles at 73° F. The data presented in Figure 6 is strongly suggestive of a simple time-temperature relationship. In Figure 7, the fatigue data have been superposed by employing the values of log a_D, determined experimentally by the construction of Figure 3. As can be seen, the superposition is remarkably good considering the normal statistical scatter of lifetime data, and defines an almost complete master fatigue curve known as an S - N curve in conventional engineering practice. Clearly, an

understanding of the implications of these types of procedures in material and engineering design will constitute a necessary step in the further progression of the science of composite materials.

B. REVERSIBLE TEMPERATURE EFFECTS

In the last section we illustrated temperature-induced processes which lead to an irreversible change in composite properties through rate processes. In this section we shall be concerned with rate processes which are reversible with changes in temperature. This area of investigation is called viscoelasticity. If we restrict ourselves to levels of stress and strain which allow the material to respond in a linear manner, we are dealing with linear viscoelasticity. It is absolutely essential that we be aware of the differentiation between reversible and irreversible phenomena. For example, if we measure the modulus of a typical cold setting unfilled epoxy at room temperature, it exhibits a modulus of roughly 300,000 psi. If, however, the temperature is increased to 200° F the modulus will be only 140,000 psi. On returning to room temperature we may regain the 300,000 psi modulus. In comparison with the earlier decomposition problem, an exposure of the material to 500 or 600° F would result in a permanent change in the structure of the material with the natural consequence that on returning to the standard temperature, the material will exhibit a modulus value which is different from the original modulus. The same remarks are equally true regarding strength properties where there can be large changes in strength due to both reversible or irreversible processes.

The normal viscoelastic response of typical organic matrix material exhibits properties paralleling the data shown in Figures 2 and 3. For example, consider the simple experiment in which we apply a step increase in length of a slender rod of our material and measure the surface traction or stress required to maintain the specimen in the extended configuration. The ratio of this stress to the computed constant strain is the relaxation modulus or time dependent Young's modulus for an isotropic material. If data are obtained as a function of time and temperature and the time dependent modulus is plotted as ordinate and log t as abscissa, then we obtain a plot very similar in appearance to Figure 2. The temperature region of rapid strength loss is denoted as the glass transition temperature and is roughly 230° F for a cold-setting epoxy. Just as with the

decomposition data, a time-temperature superposition can be employed to obtain a master curve of modulus against reduced time (log t/a_T) as in Figure 3. See for example the recent data of Kaelble (Reference 7) or Theocaris (Reference 8). For reversible viscoelastic data, the time-temperature shift distance is denoted by log a_T, and is well approximated by Equation 2. For epoxy resins below the transition temperature, ΔH is in the range of 20 K cal / mole. Thus, viscoelastic response has a much stronger temperature dependence than the decomposition reactions. More importantly, the viscoelastic data is spread out over a much larger time scale than is shown in Figure 3. While the steep descent of Figure 3 occurs in two decades, the transition in modulus due to viscoelastic processes requires twenty decades in time or more. Consequently, modulus data is represented as an exponential series

$$E(t) = \sum E_n \; e^{-t/\tau_n} \tag{5}$$

instead of a simple exponential function. The quantity τ_n is the "relaxation time" of the "nth" term of the series and is the inverse of a rate constant. Analytically, time-temperature reduction means $t/\tau_n \longrightarrow t/\tau_n a_T$. Thus, if the reduced master curve of log E (t) against log t/a_T and the analytical form of a_T is known, then the modulus is known for any other temperature.

The next problem is to relate the time-temperature dependent material properties to the constitutive equations describing time-independent response. For example, the linear elastic constitutive equation for an isotropic solid is given as

$$\sigma_{ij} = \left[K - (2/3)G\right] \Delta \delta_{ij} + 2G e_{ij} \tag{6}$$

where

δ_{ij} = 0, if $i \neq j$
= 1, if $i = j$

σ_{ij} = stress tensor
e_{ij} = stress tensor
K = bulk modulus
G = shear modulus
Δ = volumetric strain

Now we shall assume that the components of the stress and strain tensors are time dependent, and replace the material parameters K and G by time dependent material functions K (t) and G (t). If ρ (t) is a component of the stress or strain tensor, we define its Carson transform $\overset{*}{\rho}$ by the relation

$$\overset{*}{\rho} = p \int_0^\infty e^{-pt} \rho(t)\, dt \tag{7}$$

Similarly, the Carson transform $\overset{*}{m}$ (p) of a time dependent material function m (t) is defined as

$$\overset{*}{m}(p) = p \int_0^\infty e^{-pt} m(t)\, dt \tag{8}$$

The relationship involving time between the components of the stress tensor and the components of the strain tensor will now be in the form

$$\overset{*}{\sigma}_{ij} = \left[\overset{*}{K}(p) - (2/3)\overset{*}{G}(p)\right] \overset{*}{\Delta}\, \delta_{ij} + 2\overset{*}{G}(p)\, \overset{*}{e}_{ij} \tag{9}$$

This can be considered as the constitutive equation in classical linear isotropic viscoelastic theory, and is the time dependent generalization of Equation 6. To apply Equation 9 to the solution of boundary value problems, it is necessary to invert this equation. The right-hand side involves the products of Carson transforms, the inversion of which leads to a convolution integral. Thus, the inversion of Equation 9 gives

$$\sigma_{ij}(t) = \int_0^t \left\{ \left[K(t-\theta) - \frac{2}{3} G(t-\theta)\right] \frac{d\Delta(\theta)}{d\theta}\, \delta_{ij} + 2G(t-\theta)\, \frac{de_{ij}(\theta)}{d\theta} \right\} d\theta \tag{10}$$

This equation is called the superposition equation of Boltzmann. The superposition principle is of the utmost importance for the description of viscoelastic behavior under small stresses and strains. It tells how many and what kind of measurements are necessary to characterize the viscoelastic behavior completely. It tells further how the results of different forms of excitation history can be

related to each other, for instance, how we can predict the result of a dynamic stress-strain response from a creep experiment and conversely. The great power of the superposition principle lies in its generality, since it is not restricted to any special material: all its consequences remain valid independent of the micro-structure of the material under consideration. The existence of the elastic-viscoelastic correspondence principle is a direct and natural consequence of the superposition Equation 10.

Engineering stress analysis of viscoelastic materials employs the "correspondence rule," wherein transforms can be taken of the time dependent variables and forcing functions to obtain an associated elasticity problem in the transformed variables. The solution of this problem, when transformed back into real-time variables, gives the desired result, i.e., the same techniques employed in the exercise of transforming Equation 6 into Equation 10. The use of the correspondence rule is, of course, dependent upon our ability to solve the associated elasticity boundary value problem; if the elasticity solution is intractable, the viscoelastic solution will be more so. The actual mathematical details of the treatment can also be quite difficult at times. Although the above technique provides a reasonable treatment for isothermal analysis, the problem of transient thermal viscoelastic stress analysis is still without a general solution. The difficulty here is the sensitivity of viscoelastic material response to temperature which results in a simultaneous change in material properties with the transient temperature distribution through the body.

These general procedures are also applicable to anisotropic viscoelastic bodies. The details of the viscoelastic theory and stress analysis are reviewed in References 9, 10, and 11. In the appendix of this report we have outlined a procedure for closely approximating the viscoelastic response of fiber-reinforced materials by employing the results of linear elastic micromechanics and the viscoelatic analysis used in References 9 and 10. There is, unfortunately, a serious lack of reference material available at this time dealing with viscoelastic response and analysis of composite systems, with the associated critical comparison against the appropriate experimental data. Further complicating the problem is the fact that all composite systems exhibit a strong nonlinear response for which we lack the suitable analytical tools.

These nonlinearities are particularly perplexing when one attempts to develop a rigorous analysis of the ultimate properties of the system.

Just using the linear viscoelastic process greatly complicated the evaluation of the expected structural integrity of a specific design. In all instances, the rupture or failure of viscoelastic solids is strongly influenced by time-dependent phenomena (Reference 12). If we assure that it is feasible to execute a stress analysis for a given loading, specified material, type of anisotropy, and geometrical configuration, it is still necessary to combine the stress distribution with some statement of a criterion for failure. With very few exceptions, viscoelastic materials are experimentally analyzed in an uniaxial stress state. Although these efforts give invaluable information relating the rupture stress or strain to the reduced time scale t/a_T, or reduced strain or loading rate, $\frac{1}{\bar{R}\, a_T}$**, they do not provide the necessary information for the prediction of viscoelastic failure in a multiaxial stress-strain state. This becomes a serious problem, since the stress and strain distribution is multiaxial for most geometries of engineering interest. Experience with isotropic solids exhibiting very small or no time dependence does indicate that the octahedral stress or von Mises criterion can correlate uniaxial and multiaxial states; but, no such relationship has been verified for viscoelastic materials. Instead of a simple unique correlation between uniaxial and multiaxial states for a time-temperature independent body, the association of multiaxial states for viscoelastic materials must also include strain rate $\frac{1}{\bar{R}\, a_T}$ or time scale t/a_T. As a consequence there cannot be a single failure surface characterizing fracture; there is, rather, a multitude of closed surfaces, each surface characterizing the multiaxial state for a specific value of $\frac{1}{\bar{R}\, a_T}$ or t/a_T. The strength problem is particularly complicated for the anisotropic body, because workers have not, at this time, been able to experimentally verify the general multiaxial criterion of Hill (Reference 1) or others for a time-temperature independent antisotropic body.

**$\bar{R}$ = time rate factor related to $\frac{de}{dt}$ or $\frac{d\sigma}{dt}$, where $\bar{R}$ is approximately equal to time.

In addition, time dependence in the fracture process complicates the analysis of the statistics of fracture in that we must now discuss fracture in terms of a time dependent probability distribution of flaw strength as indicated in our discussion of stress corrosion. Furthermore, time dependence in material or fracture response leads to the phenomenon of fatigue or cumulative damage, wherein the lifetime of the material is a strong function of the stress-strain-temperature history of the sample or structure. In other words, how do we predict a fatigue failure from constant strain rate or constant load failure data? Finally, viscoelastic response necessarily requires energy dissipation in response to vibrational excitation. This energy dissipation can lead to large cumulative heating which can result in accelerated fatigue damage or strength loss and in some cases to chemical decomposition of the matrix materials. This phenomenon can be directly related to an interaction between the imaginary part of the complex shear modulus, or loss tangent, and the natural frequency of the design configuration. Design attention should be given to this problem when composite materials are employed in structures subjected to dynamic loads.

C. PERMEATION

Permeation of water or other agents through the matrix will have two effects on the properties of the matrix. The first effect is, for instance, that water will swell the hard glassy matrix material and accelerate rate processes. This means that the absorption of water vapor is equivalent to increasing the ambient temperature of the material, a process which is termed "plasticization" in the chemical industry technology. Thus, if we repeat our stress relaxation experiment at constant temperature but at different concentrations of water in the matrix we shall obtain data (Reference 9) similar to that in Figure 2 (where temperatures on the curve are now concentrations of the plasticizing agent). This experiment may be performed, for example, at constant temperature and differing relative humidities. Superposition of the data similar to the operation in Figure 3 can be performed with the time-plasticizer concentration parameter a_c being given as

$$\log a_c = \frac{-C_3 (1 - C/\rho_2)}{C_4 + (1 - C/\rho_2)} \qquad (11)$$

(from Reference 9), where C is the concentration of swelling agent, ρ_2 is the density of the polymeric matrix at temperature T, and C_3 and C_4 are empirical constants to be determined by the experiment. A simultaneous change in temperature and swelling agent concentration could then be approximated by the reduced time $t/a_T a_c$. Again, inducing time dependence by a swelling agent leads to a viscoelastic response which can be handled within the framework of linear viscoelasticity, and composite response can, in principle, be predicted by employing the correspondence principle (Reference 10). It is also obvious that the plasticizing effects cause a time or rate dependent decrease in ultimate properties.

The above remarks suggest that swelling of an epoxy or phenolic matrix by water can be treated in a straightforward manner; however, this is not quite true because there are additional effects which are irreversible and separate from the plasticizing action described above. The plasticizing action leads to reversible property changes, but absorption by the swelling agent and the subsequent redrying of a specimen of matrix material quite often results in permanent irreversible property loss. To understand how this irreversible loss occurs, let us examine the recent results of Alfrey, Gurnee, and Lloyd (Reference 13). In their paper they point out that hard glassy crosslinked polymers (matrix materials) when placed in contact with a solvent or swelling agent give an "anomalous" diffusion effect not explicable in terms of the Fickian process. Experimentally, one observes that as the absorbed agent penetrates into the material a sharp advancing boundary separates the inner rigid core from the outer swollen softer shell. Behind the front, which advances at constant velocity, the material seems to be in an equilibrium state with respect to swelling agent concentration. Because the swollen material forms a shell around the unswollen materials and is directly connected to the unswollen core, the core will be placed under a state of triaxial stress. A stress analysis performed on a cylindrical specimen would show (Reference 13) that the core is under a large tensile stress, which increases sharply as the swelling front advances into the material. When the swelling stresses reach a critical value in the core, a fracture occurs. In some cases this effect can be predicted analytically (Reference 13).

In addition to matrix rupture, this mechanism could also lead to the rupture of the matrix-fiber interface and, if very high swelling stresses are produced, fiber rupture may occur. Thus, we have irreversible damage inflicted by the swelling process which is clearly different from the plasticizing effect described above. Moreover, the swelling rupture of the resin and fiber-resin interface exposes the fibers to a high solvent atmosphere, which, when coupled with the swelling-induced tension in the fibers, can lead to severe stress corrosion of the reinforcement.

The above remarks would appear to explain the "water boil" tests and why these tests can inflict such extensive damage upon samples which are stored in boiling water for only a few hours. But our discussion also raises the question as to whether "water boil" is an accurate diagnostic accelerated aging test. It is a fair question to ask if the storage of a composite panel in a normal relative humidity atmosphere and at temperatures of conventional engineering interest would ever be subjected to the same apparent magnitude of internal stress as occur in the "water boil" test. In any event, the loss of composite properties due to water or swelling agent permeation of the composite matrix is a highly coupled mechanism, and much work must be done before useful analytical treatment of the various processes can become available for engineering design.

Since it appears that both large stress and strain (Reference 9) and/or permeation of water through a resin matrix produces voids, it is of interest to see whether we can predict the gross behavior of the unidirectional composite as a function of void content. It is assumed that voids are randomly distributed spherical cavities in the matrix. Then the effect of voids on the composite properties can be predicted using the properties of a degraded matrix, i.e., a porous matrix. There are a number of equations for calculating the effective stiffness and strength of a porous continuum, e.g., Mackenzie (Reference 14), Kerner (Reference 15), and Hashin (Reference 16). All theories predict various degrees of degradation as void content increases. Coble and Kingman (Reference 17) showed that the Mackenzie equation (Reference 14) agreed well with the data of sintered alumina. If we use this equation, i.e.,

$$1 - \frac{\bar{G}}{G_m} = \frac{5(3K_m + 4G_m)}{9K_m + 8G_m} P + AP^2 \qquad (12)$$

where $\bar{G}$ = shear modulus of the porous matrix; G_m, K_m = shear and bulk moduli of the pure matrix; P = volume fraction of pores in the matrix; A = a constant and assumes the matrix materials to be elastic and isotropic, then

$$\begin{aligned} K_m &= E_m / 3(1 - 2\nu_m) \\ G_m &= E_m / 2(1 + \nu_m). \end{aligned} \qquad (13)$$

By combining Equation 12 and 13, and rearranging,

$$\bar{G}/G_m = 1 - \frac{15(1 - \nu_m)}{7 - 5\nu_m} P - AP^2 \qquad (14)$$

The constant A can be determined by setting

$$\bar{G} = 0 \quad \text{when } P = 1.00 \qquad (15)$$

Furthermore, pores in the matrix can be related to the voids in the composite as follows:

$$P = v_v / v_m \qquad (16)$$

where v_v = void content in the composite, v_m = matrix content. By combining Equations 14, 15, and 16,

$$\bar{G}/G_m = 1 - \frac{15(1 - \nu_m)}{7 - 5\nu_m} \left(\frac{v_v}{v_m}\right) + \frac{8 - 10\nu_m}{7 - 5\nu_m} \left(\frac{v_v}{v_m}\right)^2 \qquad (17)$$

A comparison of this equation with experimental data reported by General Dynamics (Reference 4), reveals material properties that correspond to boron-epoxy composites, i.e.,

$$\begin{aligned} \nu_m &= 0.35 \\ v_m &= 0.38 \end{aligned} \qquad (18)$$

where it is assumed that the fiber content is 55%, and glass, 7%. It is also assumed for the purpose of comparison that the matrix material (Narmco 5505) is composed so that the ratio of the $\bar{G}/G_m$ is the same as the ratio of the

composite transverse strength to the matrix strength. With these assumptions, the theoretical prediction based on Equation 17 is shown as a solid line in Figure 9 along with the corresponding experimental data and their variations. Thus, the effect of voids on the transverse strength of unidirectional composites is quite drastic. The effect of voids on the longitudinal strength should be negligible, a fact which agrees with the measured data also reported in Reference 4. The formation of voids due to the combined action of stress and permeation will lead to a strong nonlinear viscoelastic response (Reference 9), which will be largest in the shear and transverse properties and least in the longitudinal direction of a unidirectional composite.

SECTION VI

CONCLUSION

Preliminary evidence as indicated here established the feasibility of using the conventional rate process theory, as employed in other areas of material science, for the correlation and prediction of environmental processes on the engineering response of composite structures. The mechanisms discussed should lay the groundwork for establishing a unified experimental program to define a more comprehensive and realistic evaluation of the performance of structural composites than the empirical approach.

APPENDIX

FORMULAS FOR THE ELASTIC AND VISCOELASTIC PROPERTIES OF FIBER-REINFORCED COMPOSITES

The elastic properties of these unidirectional composites are governed by a maximum of four independent macroscopic moduli, which can be computed from a generalized formula. Since material properties U_j can be separated from the geometric properties V_i in a laminated composite according to the invariant theory (Reference 18) of composite materials, a direct link between the properties of constituent materials and those of laminated composites can be calculated through a set of simple formulas.

For example, consider the stiffness matrix for orthotropic materials

$$C_{ij} = \begin{bmatrix} C_{11} & C_{12} & C_{13} & 0 & 0 & 0 \\ & C_{22} & C_{23} & 0 & 0 & 0 \\ & & C_{33} & 0 & 0 & 0 \\ & & & C_{44} & 0 & 0 \\ & & & & C_{55} & 0 \\ & & & & & C_{66} \end{bmatrix} \tag{19}$$

For transversely isotropic materials: $C_{44} = \frac{1}{2}(C_{22} - C_{23})$, $C_{22} = C_{33}$, $C_{12} = C_{13}$

For isotropic materials: $C_{11} = C_{22} = C_{33}$, $C_{12} = C_{13} = C_{23}$

$$C_{44} = C_{55} = C_{66} = \frac{1}{2}(C_{11} - C_{22})$$

In terms of a new notation proposed by Hill (Reference 19) and Hermans (Reference 20):

For fibers in square or diamond array in the 2-3 plane, Figure 9:

$$C_{ij} = \begin{bmatrix} n & \ell & \ell & 0 & 0 & 0 \\ & k+m & k-m & 0 & 0 & 0 \\ & & k+m & 0 & 0 & 0 \\ & & & \gamma & 0 & 0 \\ & & & & \mu & 0 \\ & & & & & \mu \end{bmatrix} \tag{20}$$

For fibers in hexagonal or "random" array in 2-3 plane:

$$\gamma = m \tag{21}$$

Hill showed that for any fiber array having two planes of identical symmetry in the 2-3 plane, i.e., $C_{22} = C_{33}$, $\bar{n}$ and $\bar{\ell}$ are dependent on $\bar{k}$. This can be seen in the triaxial loadings illustrated in Figure 10. Thus,

a) If $\epsilon_3 = 0$ (plane strain), $\frac{\sigma_3}{p} = \bar{\ell}\,\frac{\sigma_3}{p}\bar{k}$

b) If $\epsilon_1 + \epsilon_2 = 0$ (uniaxial extension), $\frac{\sigma_3}{p} = \frac{\bar{n}}{\ell}\ \bar{n} = \frac{\sigma_3}{p}\ \bar{\ell}$

Through simple algebraic operations, the following relations can be obtained:

$$\bar{\ell} = V_f \ell_f + V_m \ell_m + \frac{\ell_f - \ell_m}{k_f - k_m}\,(\bar{k} - V_f k_f - V_m k_m) \tag{22}$$

$$\bar{n} = V_f n_f + V_m n_m + \left[\frac{\ell_f - \ell_m}{k_f - k_m}\right]^2 (\bar{k} - V_f k_f - V_m k_m) \tag{23}$$

$$\overline{V_{12}} = \frac{\bar{\ell}}{2\bar{k}} = V_f \nu_f + V_m \nu_m + \left[\frac{\nu_f \nu_m}{\frac{1}{k_f} - \frac{1}{k_m}}\right]\left(\frac{1}{\bar{k}} - \frac{V_f}{k_f} - \frac{V_m}{k_m}\right) \tag{24}$$

$$\bar{E}_{11} = \bar{n} - \frac{\bar{\ell}^2}{2\bar{k}} = V_f E_f + V_m E_m - 4\left[\frac{\nu_f - \nu_m}{\frac{1}{k_f} - \frac{1}{k_m}}\right]^2 \left(\frac{1}{\bar{k}} - \frac{V_f}{k_f} - \frac{V_m}{k_m}\right) \tag{25}$$

Thus, once $\overline{k}$ is found for a unidirectional composite, $\overline{\ell}$ and $\overline{n}$, or, equivalently, $\overline{\nu}_{12}$ and $\overline{E}_{11}$, can be found.

The number of independent composite moduli are <u>three</u> for transversely isotropic composite, and <u>four</u> for orthotropic composites.

For orthotropic materials, the following relations exist:

(They apply to both constituent and composite moduli.)

New Moduli	C_{ij}	Engineering Constants
k(plane strain bulk modulus	$\frac{1}{2}(C_{22} + C_{23})$	$\frac{E_{22}}{2(1-\nu_{23}-2\nu_{21}\nu_{12})}$
ℓ	$C_{12} = C_{13}$	$\frac{\nu_{21} E_{11}}{1-\nu_{23}-2\nu_{21}\nu_{12}} = \frac{\nu_{12} E_{22}}{1-\nu_{23}-2\nu_{21}\nu_{12}}$
n	C_{11}	$\frac{E_{22}}{2(1+\nu_{23})}$
m(shear modulus at $\pi/4$ from principal axes)	$\frac{1}{2}(C_{22}-C_{23})$	$\frac{E_{22}}{2(1+\nu_{23})}$
γ(transverse shear modulus)	C_{44}	G_{23}
μ(longitudinal shear modulus)	$C_{55} = C_{66}$	G_{12}
$n - \frac{\ell^2}{k}$	$C_{11} - \frac{2C_{12}^2}{C_{22}+C_{23}}$	E_{11}
$\frac{4(nk-\ell^2)m}{(k+m)n-\ell^2}$	$\frac{[C_{11}(C_{22}+C_{23})-2C_{12}^2](C_{22}-C_{23})}{C_{11}C_{22}-C_{12}^2}$	E_{22}
$\frac{\ell}{2k}$	$\frac{C_{12}}{C_{22}+C_{23}}$	ν_{12}

$$\frac{2m\ell}{(k+m)n-\ell^2} \qquad \frac{C_{12}(C_{22}-C_{23})}{C_{11}C_{22}-C_{12}^2} \qquad \nu_{21}$$

$$\frac{(k-m)n-\ell^2}{(k+m)n-\ell^2} \qquad \frac{C_{11}C_{23}-C_{12}^2}{C_{11}C_{22}-C_{12}^2} \qquad \nu_{23}$$

For transversely isotropic materials mathematical relationships are the same as above except that $\gamma = m$. All the relations above can be applied to both constituent and composite properties; bars are used to denote composite properties, and subscripts f and m denote fibers (or fillers) or matrix, respectively.

For isotropic materials, same as above except

$$k + m = n \qquad k - m = \ell \qquad \gamma = n = \mu$$

The relationships in terms of isotropic constants E and ν are:

$$\begin{aligned} k &= \frac{E}{2(1+\nu)(1-2\nu)} \\ \ell &= \frac{\nu E}{(1+\nu)(1-2\nu)} = 2\nu k \\ n &= \frac{(1-\nu)E}{(1+\nu)(1-2\nu)} = 2(1-\nu)k \\ m &= \gamma = \mu = \frac{E}{2(1+\nu)} = G = (1-2\nu)k \end{aligned} \tag{26}$$

If fibers are transversely isotropic, e.g., Thornel fibers, the following formulas shoud be used for the computation of the new symbols:

$$\begin{aligned} k &= \frac{E_{22}}{2(1-\nu_{23}-2\nu_{21}\nu_{12})} \\ \ell &= 2\nu_{12}k, \quad n = 2(1-\nu_{23})\frac{E_{11}}{E_{22}}k \\ m &= \frac{1-\nu_{23}-2\nu_{21}\nu_{12}}{1+\nu_{23}}k, \quad \mu = G_{12} \end{aligned} \tag{27}$$

Using the following material properties of the constituents:

Material	Epoxy	Glass	Boron	Graphite (Thornel 40)
E_{11}	0.5×10^6 psi	10.6×10^6 psi	60×10^6 psi	40×10^6 psi
E_{22}	0.5×10^6 psi	10.6×10^6 psi	60×10^6 psi	1.5×10^6 psi
ν_{12}	0.35	0.22	0.2	0.2
ν_{23}	0.35	0.22	0.2	0.2
G_{12}	0.185×10^6 psi	4.34×10^6 psi	25×10^6 psi	4×10^6 psi

The numerical values of the new symbols are:

Material	Epoxy (psi)	Glass (psi)	Boron (psi)	Thornel 40 (psi)
k	0.617×10^6	7.78×10^6	41.67×10^6	3.47×10^6
(k/k_m)		(12.6)	(67.5)	(5.62)
ℓ	0.432×10^6	3.41×10^6	16.67×10^6	1.39×10^6
(ℓ/ℓ_m)		(7.9)	(38.6)	(3.21)
n	0.802×10^6	12.1×10^6	66.67×10^6	44.44×10^6
(n/n_m)		(15.1)	(83.1)	(55.42)
$m = \gamma$	0.185×10^6	4.34×10^6	25.0×10^6	2.08×10^6
(m/m_m)		(23.8)	(135.1)	(11.26)
μ	0.185×10^6	4.34×10^6	25.0×10^6	5.0×10^6
(μ/μ_m)		(23.8)	(135.1)	(27.02)

Quantities in parentheses are normalized properties in terms of epoxy.

The composite moduli for a macroscopically transversely isotropic material, i.e., $\bar{k}$, $\bar{m}$, and $\bar{\mu}$ ($\bar{\gamma} = \bar{m}$), can be expressed in terms of the constituent properties as follows (after Hermans):

$$\bar{k} = \frac{k_m(k_f + m_m)V_m + k_f(k_m + m_m)V_f}{(k_f + m_m)V_m + (k_m + m_m)V_f} \tag{28}$$

$$\bar{m} = m_m \frac{2V_f m_f(k_m + m_m) + 2V_m m_f m_m + V_m k_m(m_f + m_m)}{2V_f m_m(k_m + m_m) + 2V_m m_f m_m + V_m k_m(m_f + m_m)} = \bar{\gamma} \tag{29}$$

$$\bar{\mu} = \frac{(\mu_f + \mu_m)\mu_m V_m + 2\mu_f \mu_m V_f}{(\mu_f + \mu_m)V_m + 2\mu_m V_f} \tag{30}$$

The mathematical model used consists of concentric cylinders surrounded by an unbounded composite.

These formulas can be rearranged to conform to a generalized formula as follows:

$$\frac{\bar{P}}{P_m} = \frac{1+\zeta\eta V_f}{1-\eta V_f} \tag{31}$$

where

$$\eta = \frac{\frac{P_f}{P_m} - 1}{\frac{P_f}{P_m} + \zeta} = \frac{\gamma - 1}{\gamma + \zeta} \tag{32}$$

$\bar{p}$ = a composite modulus, $\bar{k}$, $\bar{m}$, or $\bar{\mu}$;

p_f = corresponding fiber modulus, k_f, m_f, or μ_f, respectively;

p_m = corresponding matrix modulus, k_m, m_m, or μ_m, respectively;

ζ = a measure of reinforcement and depends on boundary conditions (the geometries of inclusions and loading conditions).

The elastic moduli for particulate (spherical inclusions) composites can also be reduced to one generalized formula. The original formula derived by Kerner and Hashin are:

$$\bar{K} = \frac{\frac{K_m V_m}{3K_m + 4G_m} + \frac{K_f V_f}{3K_f + 4G_m}}{\frac{V_m}{3K_m + 4G_m} + \frac{V_f}{3K_f + 4G_m}} \tag{33}$$

$$\bar{G} = G_m \frac{\frac{V_f G_f}{(7-5V_m)G_m + (8-10V_m)G_f} + \frac{V_m}{15(1-V_m)}}{\frac{V_f G_m}{(7-5V_m)G_m + (8-10V_m)G_f} + \frac{V_m}{15(1-V_m)}} \tag{34}$$

The composite moduli for hollow-fiber-reinforced unidirectional composites, derived in Reference 16, can also be arranged to fit out generalized formula, except that instead of γ being the ratio of p_f/p_m, the following corrections must be made:

$$(1)\ \text{For } \bar{k} = K_{23} \qquad \gamma = \frac{1-\alpha^2}{1+\frac{\alpha^2}{1-2V_f}} \frac{K_f}{K_m}$$

$$(2)\ \text{For } \bar{\mu} = G \qquad \gamma = \frac{1-\alpha^2}{1+\alpha^2} \frac{G_f}{G_m} \tag{35}$$

where α is the ratio of the inside and outside radii of the hollow fiber. For dilute composites, the generalized formula can be expanded into a power series:

$$\frac{\bar{p}}{p_m} = 1 + (1+\zeta)\eta V_f [1 + \eta V_f + (\eta V_f)^2 + \cdots] \tag{36}$$

$$= 1 + (1+\zeta)\eta V_f + O(\eta V_f)^2 \tag{37}$$

$$\frac{\bar{p}}{p_m} \cong 1 + (1+\zeta)\eta V_f \tag{38}$$

This can be called the generalized Einstein's equation. If the inclusions are rigid, i.e.,

$$\frac{p_f}{p_m} = \infty, \text{ then } \eta = 1, \text{ and}$$

the matrix is incompressible, i.e.,

$$V_m = \frac{1}{2}, \text{ and } \zeta = \frac{3}{2} \text{ for } \bar{G}$$

so that

$$\frac{\bar{G}}{G_m} = 1 + \frac{5}{2} V_f \tag{39}$$

This is the Einstein's original equation, intended for the viscosity of dilute suspension.

The limiting values of η are:

(1) For rigid inclusions, $\eta = 1$

(2) For homogeneous material, $\eta = 0$

(3) For voids, $p_f/p_m = 0$, then $\eta = -1/\zeta$

The limiting values of ζ are:

$$(1)\ \zeta = 0,\ \frac{\bar{p}}{p_m} = \frac{1}{1-\eta V_f} = \frac{1}{p_m\left(\frac{V_f}{p_f} + \frac{V_m}{p_m}\right)}$$

$$\frac{1}{\bar{p}} = \frac{V_f}{p_f} + \frac{V_m}{p_m} \tag{40}$$

This is the series-connected model which gives the lower bound of a composite modulus.

$$(2)\ \zeta = \infty,\ \eta = 0$$

$$\zeta\eta = \frac{p_f}{p_m} \cdot 1 \tag{41}$$

$$\frac{\bar{p}}{p_m} = p_f V_f + p_m V_m$$

This is the parallel-connected model, which gives the upper bound. Thus, ζ is regarded as a measure of reinforcement which covers the entire possible range of composite moduli as ζ goes from zero to infinity. Once the ζ factors are known, the composite elastic moduli for fiber and particulate composites are determined from the generalized formula.

Further simplifications can be made for purposes of interpolation from existing micromechanics calculations by directly employing the engineering constants E_f, E_m, V_f, V_m, G_f, and G_m for p_f and p_m in Equations 31 and 32. Thus $\bar{p}$ would yield directly an estimate of E_{22}, G_{12}, and V_{23}. Within the spirit of these approximations one may obtain reasonable estimates of the composite elastic coefficients as follows:

$$E_{11} \cong E_f V_f + E_m V_\eta \tag{42}$$

$$V_{12} \cong V_f V_f + V_m V_m \tag{43}$$

with

$$G_{12}/G_m\ ,\ E_{12}/E_m\ ,\text{and}\ V_{23}/V_m$$

being obtained from Equations 31 and 32 by the direct substitution of the appropriate engineering constants for p_f/p_m. Reliable estimates for the ζ factor can be obtained by comparison of Equations 31 and 32 with the numerical micromechanics solutions employing formal elasticity theory. For example, Figures 11 and 12 show the predictions of Equations 31 and 32 for various reinforcements/matrix stiffnesses and is compared with the results of Adams, Doner, and Thomas (Reference 21). The approximate formula duplicates their results for all ratios of p_f/p_m. In Figures 13 and 14 we have a comparison of the dependence of composite moduli, based upon Foye's calculations (Reference 22), as a function of volume fraction for square fibers in a diamond array. For the predictions of shear G_{12}, $\zeta_G = 1$ and for stiffness E_{22}, $\zeta_E = 2$ for the calculations shown in Figures 11 - 14. In Figures 15 we show the results of our generalized formula compared with the results of different micromechanics calculations. Note that our approximate formula provides a good correlation with Foye's computations for hexagonal array of circular fibers up to $v_f = 65\%$. At higher volume fractions the results lie between the hexagonal and the square arrays. Although there is some disparity between the results of formal analysis and our results, in practical cases one does not employ high volume fractions of fibers, $v_f > 70\%$, due to the impairment of the strength properties.

Further confidence can be gained in this interpolation procedure by returning to Figures 13 and 14 and examining the dependence of the transverse stiffness moduli and the longitudinal-transverse shear moduli upon increasing aspect ratio for square filaments (Reference 23). The factors ζ_E and ζ_G are functions of the width thickness ratios and were found to be of the form:

$$\zeta_E = 2(a/b)$$

and

$$\log \zeta_G = \sqrt{3} \log (a/b)$$

These ζ factors were determined by fitting Foye's results and are represented in graphical form in Figure 16. Results in Figures 13 and 14 indicate good agreement between our approximate formulas and elasticity calculations for different aspect ratios and volume fractions. These results allow the extension of the limited elasticity calculations to the prediction of, for example, the dependence of the moduli, E_{22} and G_{12}, on aspect ratio, reinforcement stiffness/matrix stiffness and volume fraction loading as illustrated in Figures 17 and 18.

On the premise that our model is a reasonable model for the determination of composite moduli, closed form relations between the constituent moduli and the composite moduli of laminated composites can now be derived. As shown in Reference 18 on the invariant properties of composites, the elastic properties of unidirectional AND laminated composites are governed by U_1, U_2, U_3, U_4, and U_5, and the lamina orientations as a function of z, i.e., $\theta = \theta(z)$. The following relations are needed:

$$U_1 = (3Q_{11} + 3Q_{22} + 2Q_{12} + 4Q_{66})/8$$

$$U_2 = (Q_{11} - Q_{22})/8$$

$$U_3 = (Q_{11} + Q_{22} - 2Q_{12} - 4Q_{66})/8$$

$$U_4 = (Q_{11} + Q_{22} - 6Q_{12} - 4Q_{66})/8$$

$$U_5 = (Q_{11} + Q_{22} - 2Q_{12} + 4Q_{66})/8$$

for an orthotropic material. The components of Q_{ij} can be expressed in terms of engineering constants if and only if Q_{ij} is orthotropic:

$$Q_{11} = E_{11}/(1-\nu_{12}\nu_{21})$$

$$Q_{22} = E_{22}/(1-\nu_{12}\nu_{21})$$

$$Q_{12} = \nu_{12} Q_{22} = \nu_{21} Q_{11}$$

$$Q_{66} = G_{12}$$

Thus, for example, the stiffness matrix for an angle ply composite having an angle ply angle (2α) and any orientation angle ϕ of the principal areas of the laminate and the coordinate area of the applied stress can be evaluated as

$$A'_{11} = U_1 + U_2 \cos 2\alpha \cos 2\phi + U_3 \cos 4\alpha \cos 4\phi$$
$$A'_{22} = U_1 - U_2 \cos 2\alpha \cos 2\phi + U_3 \cos 4\alpha \cos 4\phi$$
$$A'_{12} = U_4 - U_4 \cos 4\alpha \cos 4\phi$$
$$A'_{66} = U_5 - U_3 \cos 4\alpha \cos 4\phi$$
$$A'_{16} = -\frac{1}{2} U_2 \cos 2\alpha \sin 2\phi - U_3 \cos 4\alpha \sin 4\phi$$
$$A'_{26} = -\frac{1}{2} U_2 \cos 2\alpha \sin 2\phi + U_3 \cos 4\alpha \sin 4\phi$$

The inversion of A_{ij} yields the engineering constants for the angle ply.

By using this approximate procedure for predicting moduli, elasticity relations between the constituent and composite properties can be expressed in a generalized formula. Designers can now make exact calculations, without using computers, relating the constituent properties directly to the elastic constants of a laminated composite. Both constitutent materials may be transversely isotropic. Designers can now assess the contribution of V_f, p_f/p_m, and the reinforcing factor ζ to the composite moduli directly.

These results may be extended to viscoelastic computations by taking advantage of the very accurate approximation of direct substitution of p_m (t/a_T) values as pointed out by Schapery.

REFERENCES

1. R. Hill, Mathematical Theory of Plasticity, Oxford University Press (1950).

2. V. D. Azzi and S. W. Tsai, "Anisotropic Strength of Composites," Experimental Mechanics, (Sept. 1965).

3. K. H. Boller, Strength Properties of Reinforced Plastic Laminates at Elevated Temperatures, Wright Air Development Center Tech. Report 59-569 (1960).

4. Fort Worth Division of General Dynamics, Structural Airframe Application of Advanced Composite Materials, Air Force Materials Laboratory Contract No. AF 33(615)-5257, Third Quarterly Progress Report, March 1967.

5. J. C. Halpin, Unpublished results.

6. G. H. Stevens, Fatigue Tests of Phenolic Laminate at High Stress Levels and Elevated Temperatures, Forest Products Lab Report No. 1884 (1961).

7. Kaelble, D. H., "Dynamic and Tensile Properties of Epoxy Resins," J. Appl. Poly. Sci., Vol 9, p. 1213 (1965).

8. P. S. Theocaris, Rheology ACTA, Vol 2, p. 92, (1962).

9. J. C. Halpin, "Introduction to Viscoelasticity" in Composite Materials Workshop, Edited by S. W. Tsai, J. C. Halpin, and N. J. Pagano, Technomic Publishing Co., Inc., Stamford, Conn., (1967).

10. R. A. Schapery, "Stress Analysis of Viscoelastic Composite Materials," in Composite Materials Workshop, Edited by S. W. Tsai, J. C. Halpin, and N. J. Pagano, Technomic Publishing Co., Inc. Stamford, Conn. (1967).

11. Harry H. Hilton, "Viscoelastic Analysis," in Engineering Design for Plastics, Edited by Eric Baer, Reinhold Publishing, New York, New York (1964).

12. J. C. Halpin, J. Composite Materials, Vol. 1, p. 64 (1967); J. C. Halpin and Gerhard Jacoby, "Fracture of Amorphous Polymeric Solids," Maco Molecular Reviews, Edited by Peterlin, Zimm, and Goodman, Interscience, New York, New York (1968).

13. Tumer Alfrey, Jr., E. F. Gurnee, and W. G. Lloyd, "Diffusion in Glass Polymers," J. Polymer Science Part C, Vol. 12, p. 249 (1966).

14. J. K. Mackenzie, J. Proc. Phy. Soc. (London), Vol. 63B, p. 2 (1956).

15. E. H. Kerner, J. Proc. Phy. Soc. (London), Vol. 69B, p. 802 (1956); Vol. 69 B, p. 808 (1956).

16. Z. Hashin, Bull. Res. Council, Israel, Vol. 56, p. 46 (1955).

17. R. L. Coble, and W. D. Kingman, J. Am. Ceram. Soc., Vol. 39, p. 377 (1956).

18. S. W. Tsai and N. J. Pagano, "Invariant Properties of Composite Materials" in Composite Materials Workshop edited by Tsai, Halpin, and Pagano, Technomic Publishing, Stamford, Conn. (1968).

19. R. Hill, "Theory of Mechanical Properties of Fiber-Strengthened Materials: I. Elastic Behavior, "J. Mech. Phys. Solids, Vol. 12, (1964) p. 199.

20. J. J. Hermans, "The Elastic Properties of Fiber Reinforced Materials When the Fibers are Aligned," Proc. Konigl. Nederl. Akad Weteschappen Amsterdam, Vol. B70, No. 1 (1967), p. 1.

21. D. F. Adams, and D. R. Doner, and R. L. Thomas, AFML TR 67-96.

22. R. L. Foye, "Structural Composites," Quarterly Progress Report No. 2, AFML Contract No. AF 33(613)-5150 (1966).

23. J. C. Halpin, and R. L. Thomas, J. Composit. Mat. 2, Oct. (1968).

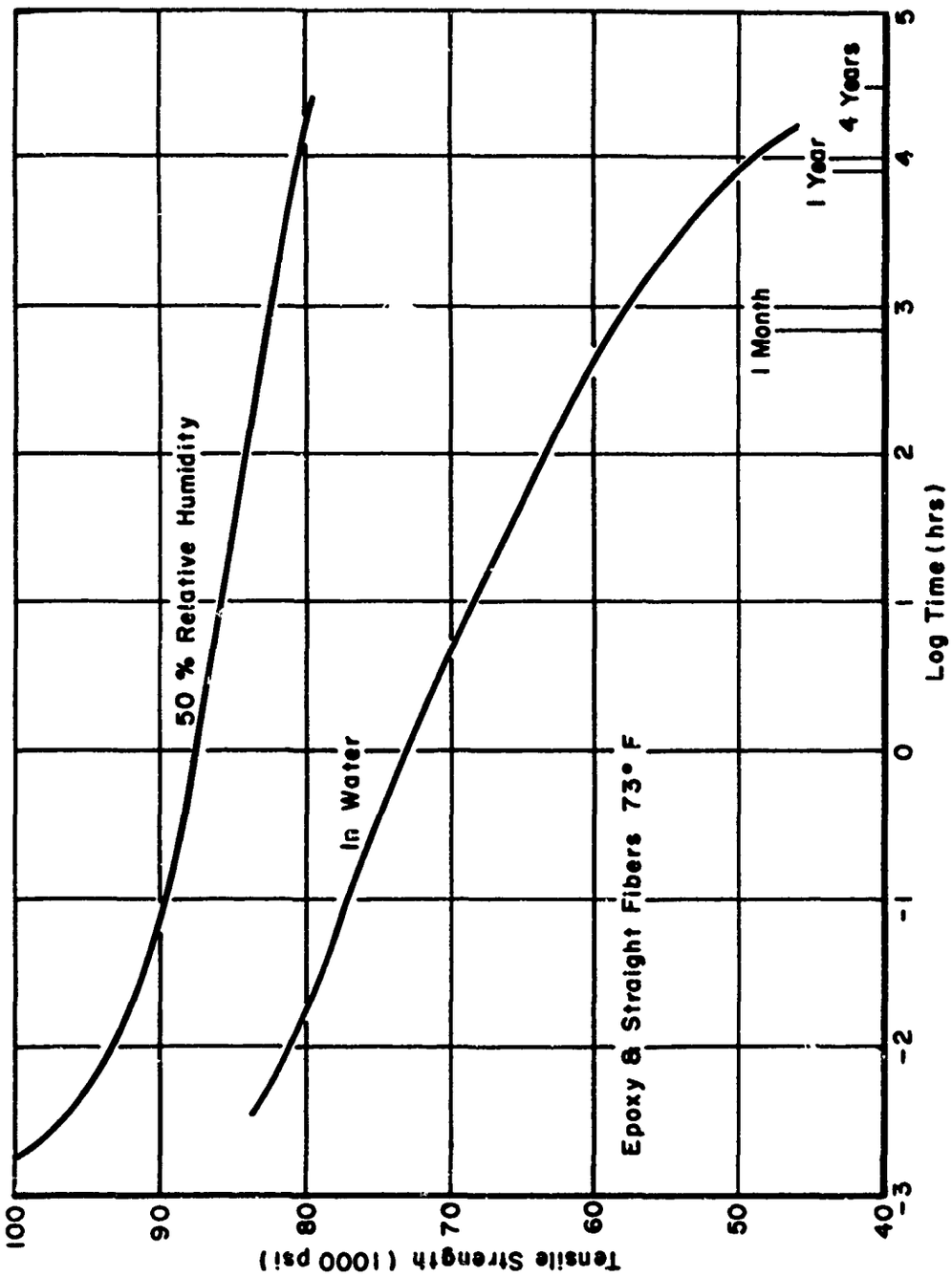

Figure 1. Stress Rupture Data of "Boller" for a Laminated Composite of Undirectional Glass-Epoxy Plates in Different Water Environments.

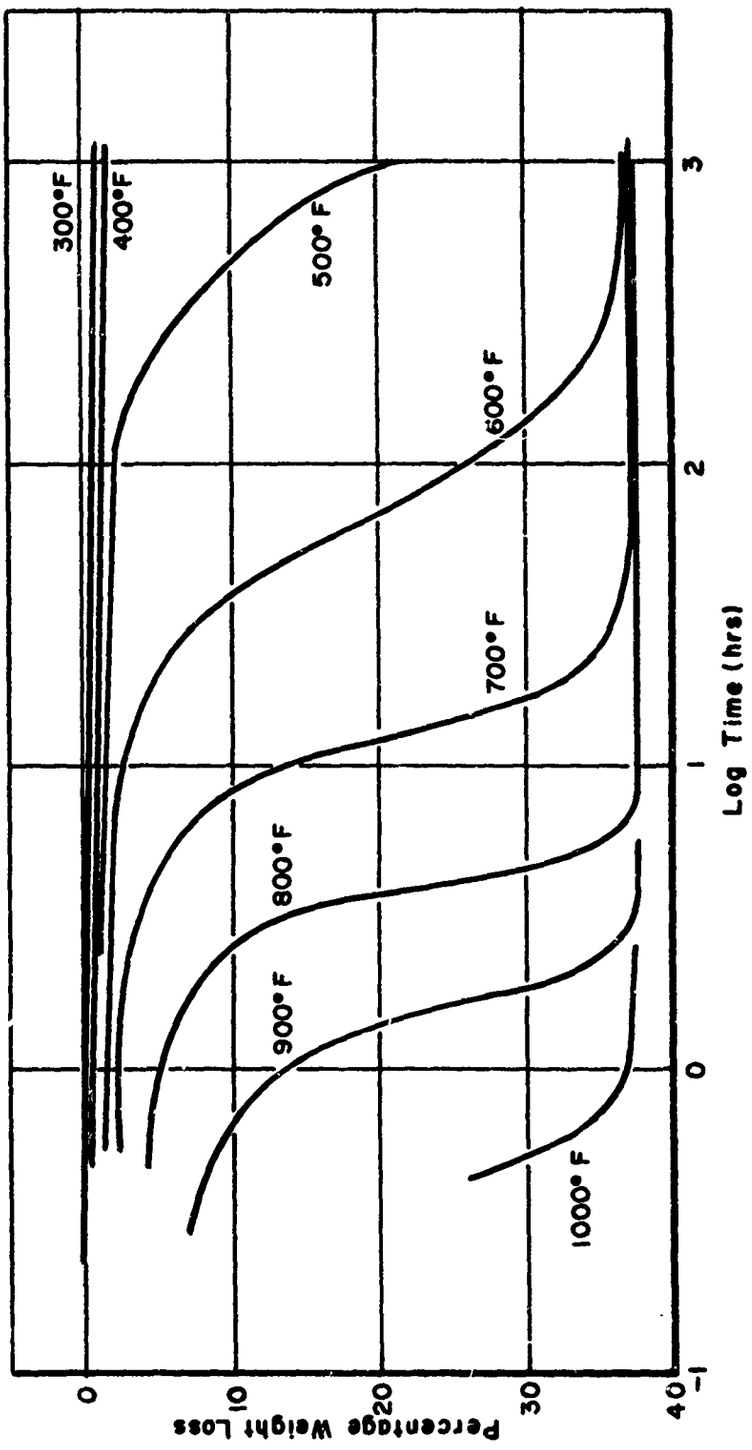

Figure 2. Deterioration as Weight Loss at Elevated Temperatures for Glass-Fiber Phenolic Laminates

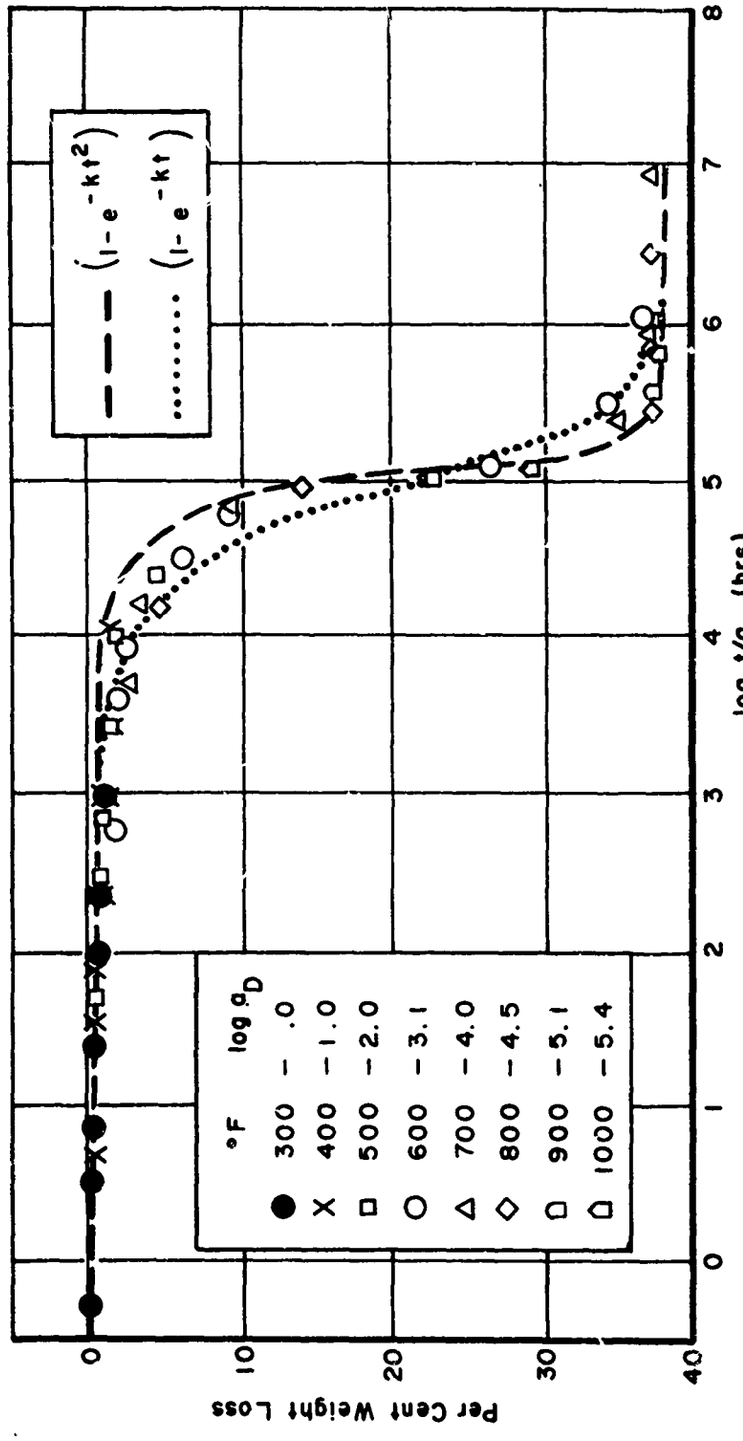

Figure 3. Master Curve of Weight Loss vs. Reduced Time Constructed (from the Earlier Figure) Employing the Log a_D Terms on the Graph

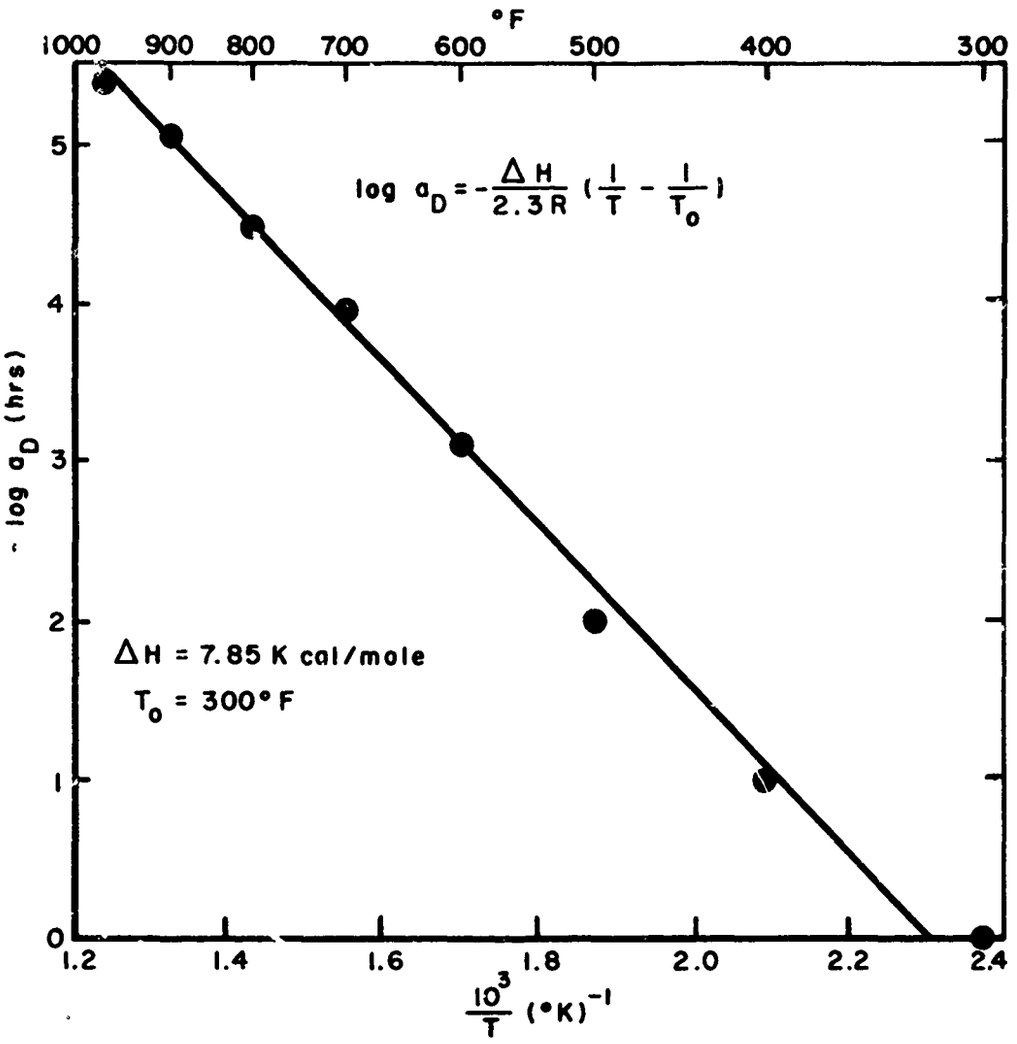

Figure 4. Determination of the Activation Energy from an Arrhenius Plot of the Shift Factors Determined (in Earlier Figure)

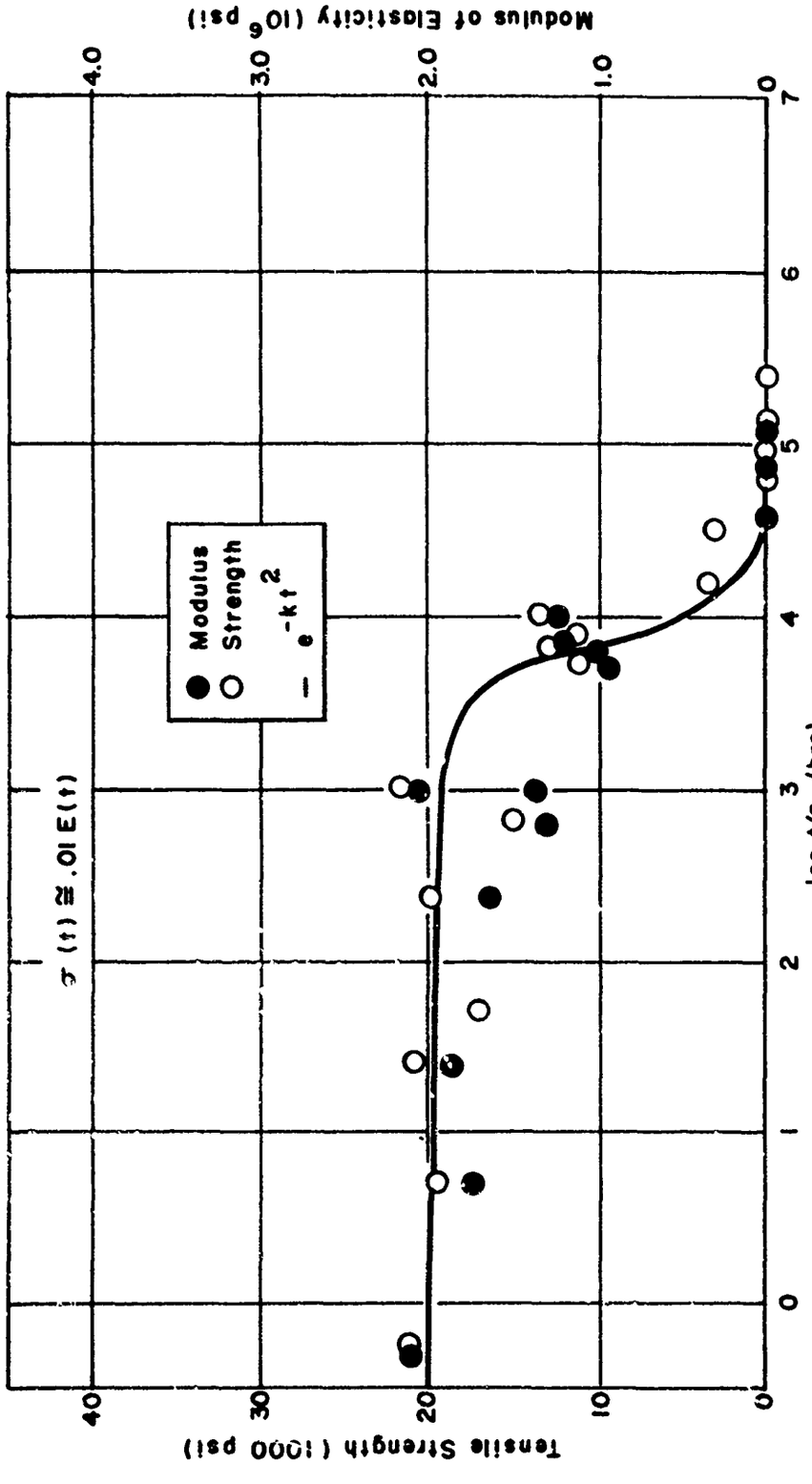

Figure 5. Composite Curves of the Modulus and Strength for the Phenolic Glass Composite Against Reduced Time During the Degradation Reaction

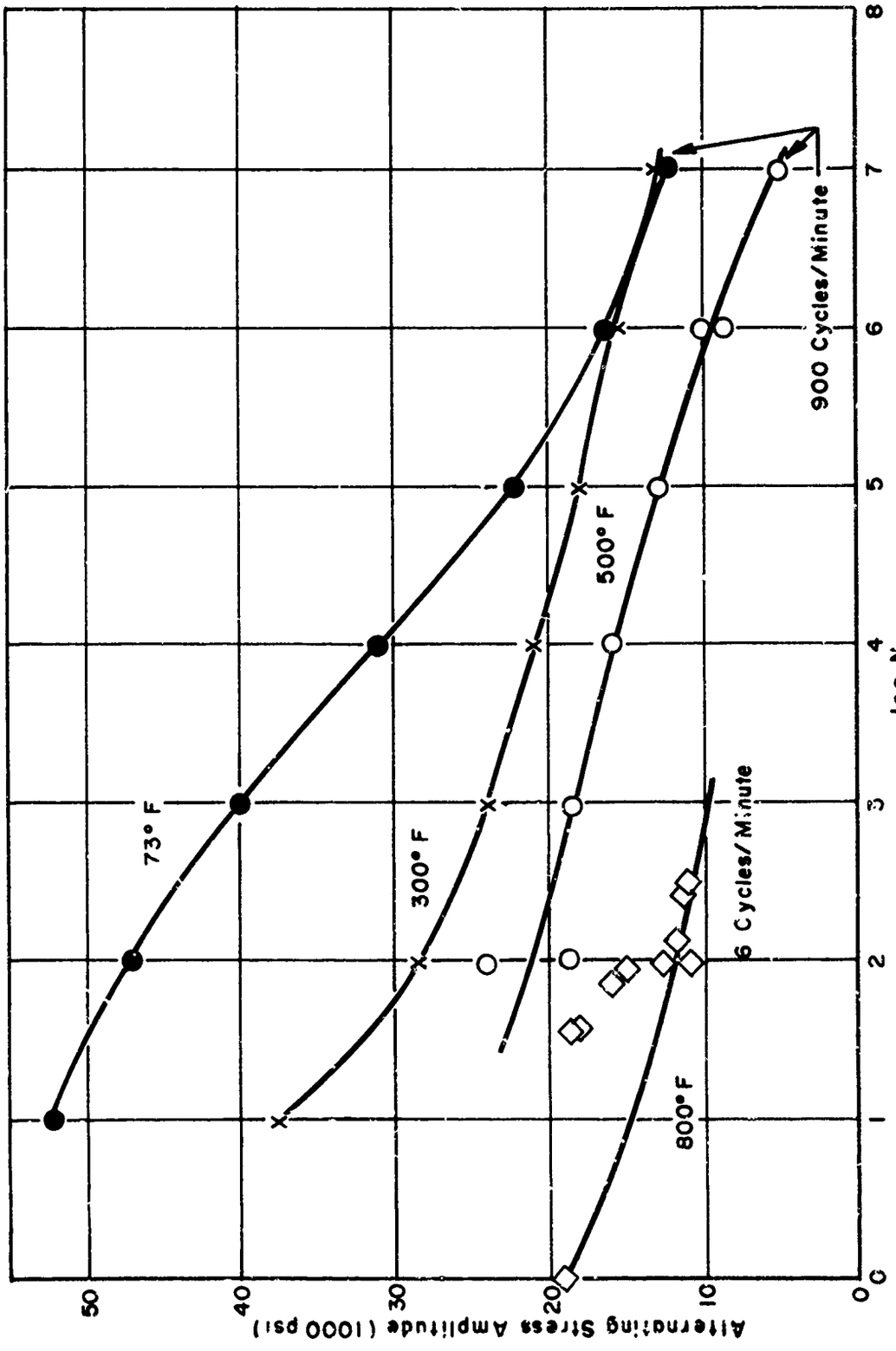

Figure 6. Fatigue Curves for Phenolic Resin Glass Composite Determined at Various Temperatures

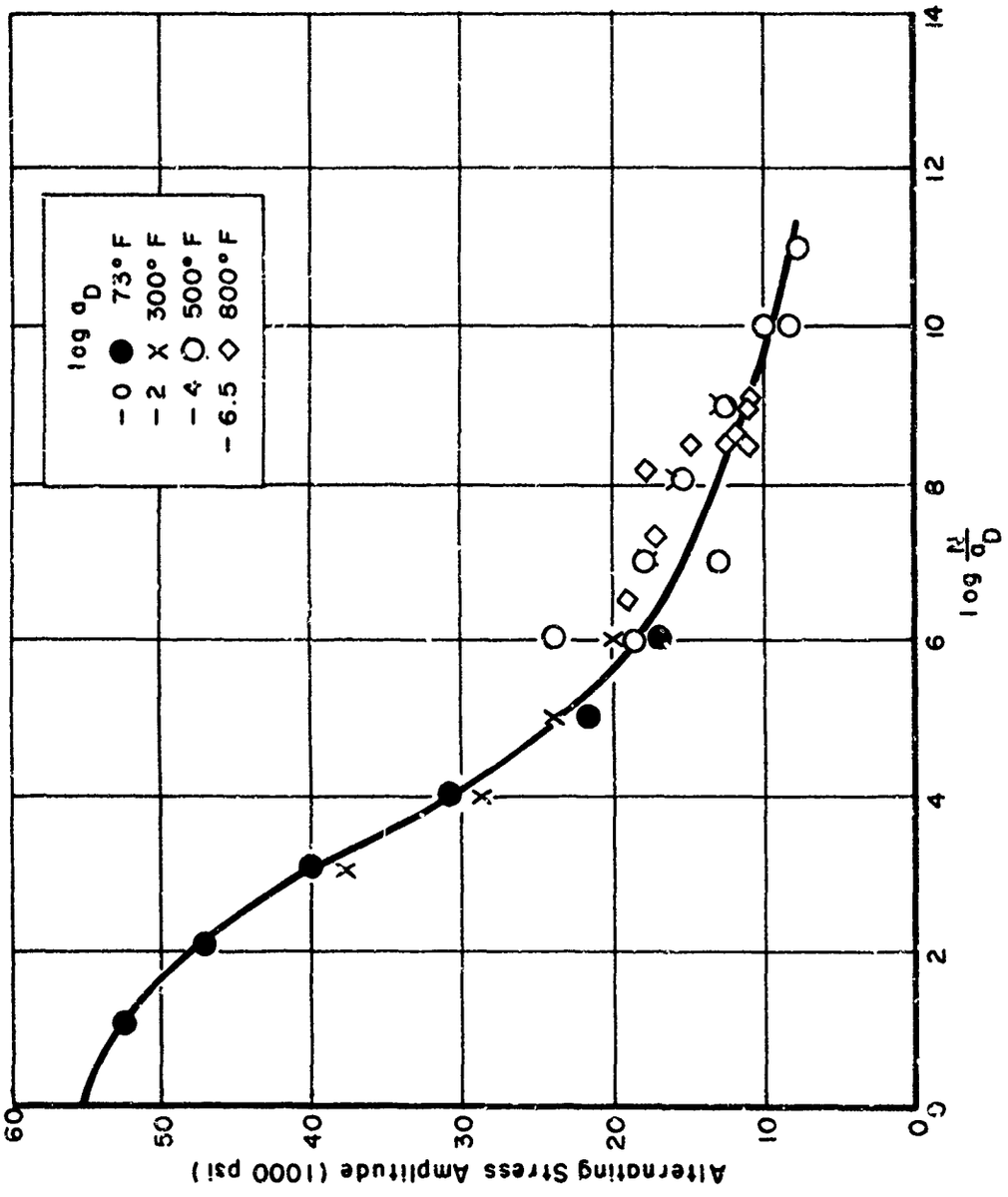

Figure 7. Fatigue Master Curve Constructed With the Same Shift Factors, Log a_D, as Employed in Figure 4

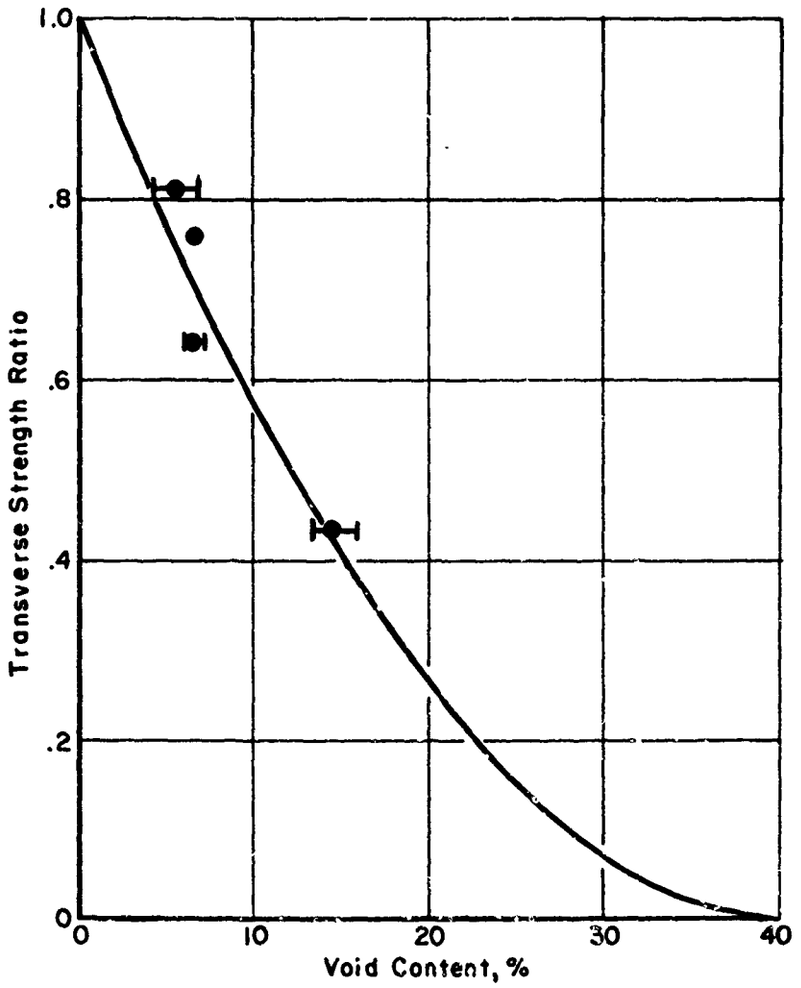

Figure 8. Dependence of Transverse Strength Ration on Void Content of Boron Epoxy Composite

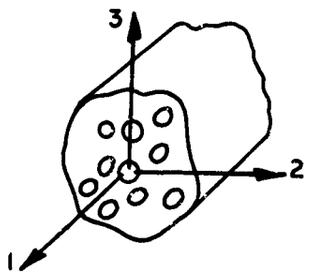

Figure 9. Illustration of Coordinate Axes for a Transversely Isotropic Composite

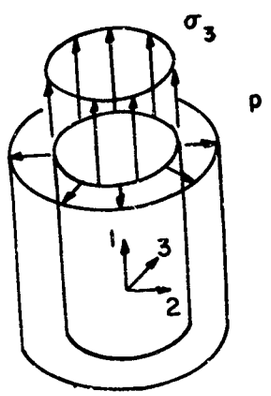

Figure 10. Illustration of Hydrostatic Pressure Applied to Fiber Reinforced Material

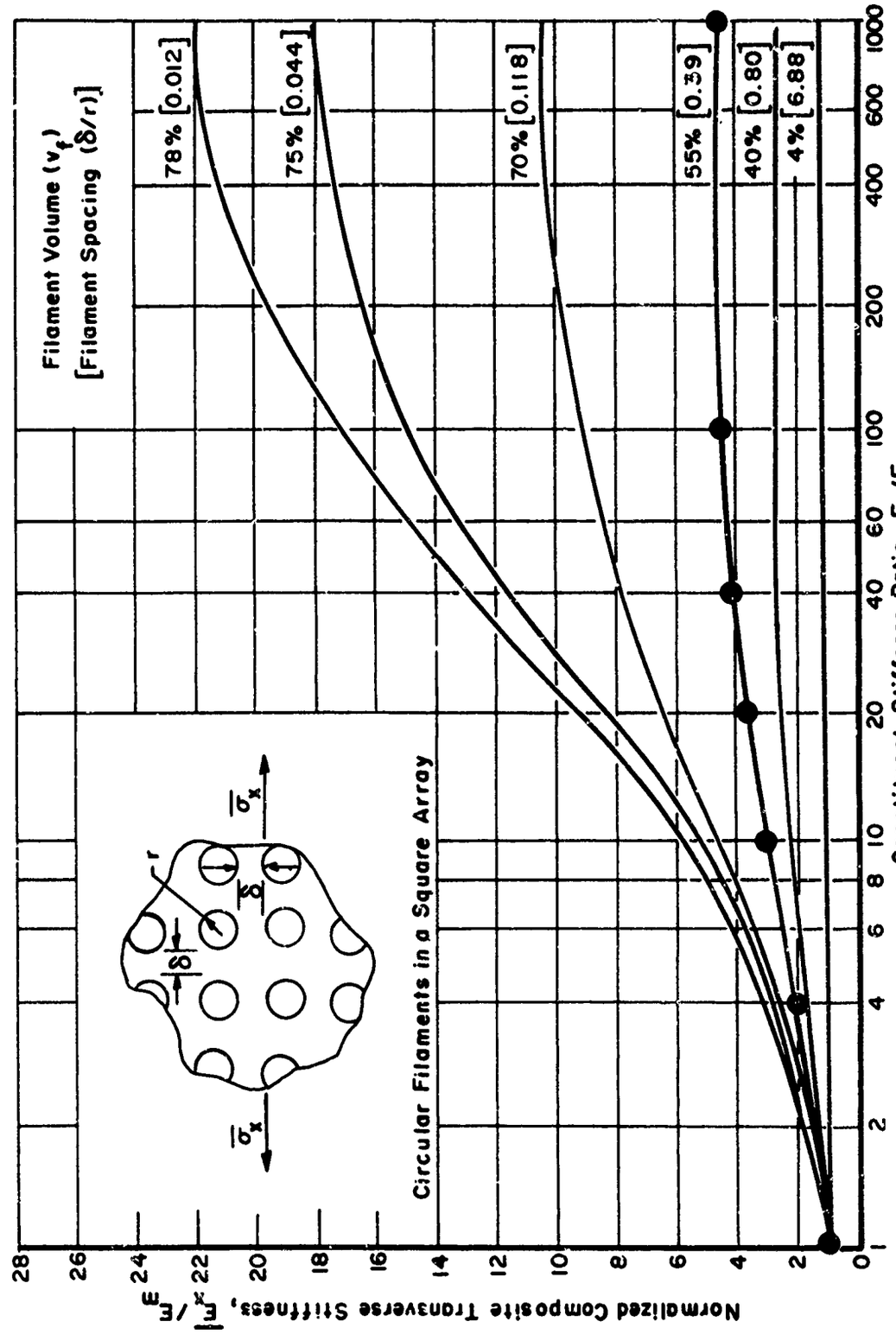

Figure 11. Comparison of Equations 31 and 32 with Finite Element Analysis of Normalized Composite Transverse Stiffness (Circular Fibers)

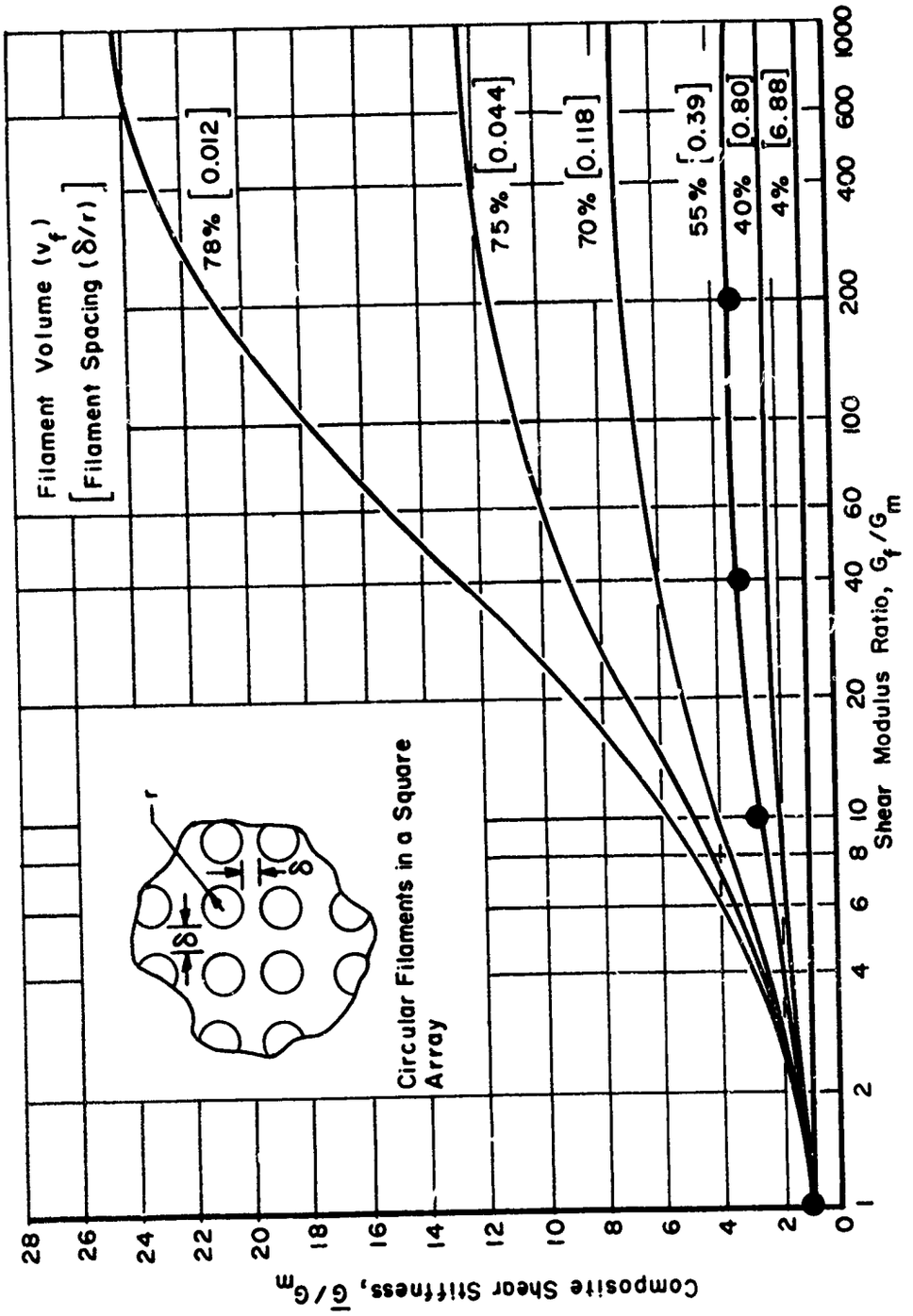

Figure 12. Comparison of Equations 31 and 32 with Finite Element Analysis of Normalized Composite Shear Loading (Circular Fibers)

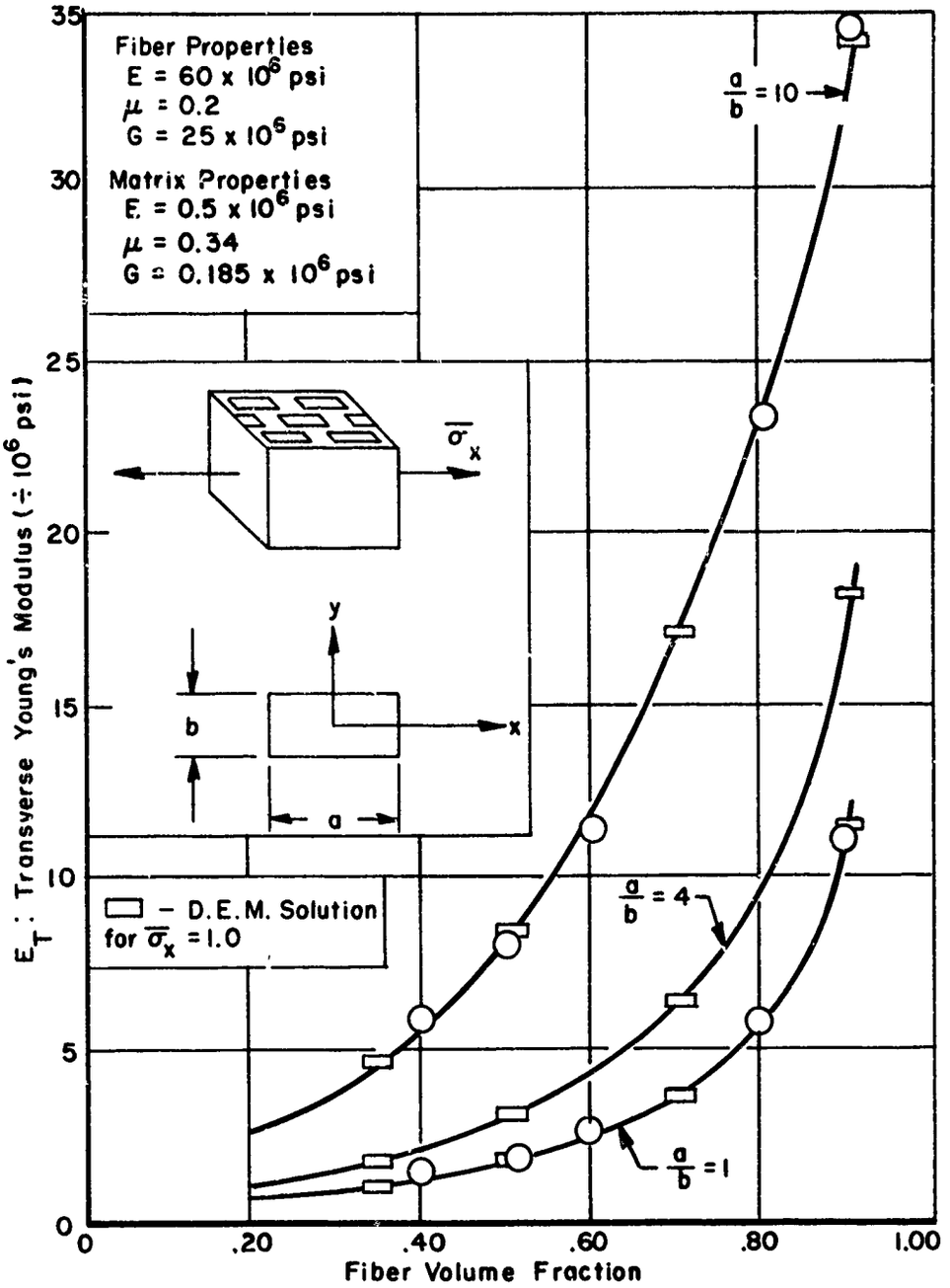

Figure 13. Comparison of Equations 31 and 32 with Finite Element Analysis of Transverse Modulus of Composites Containing Rectangularly Shaped Fibers

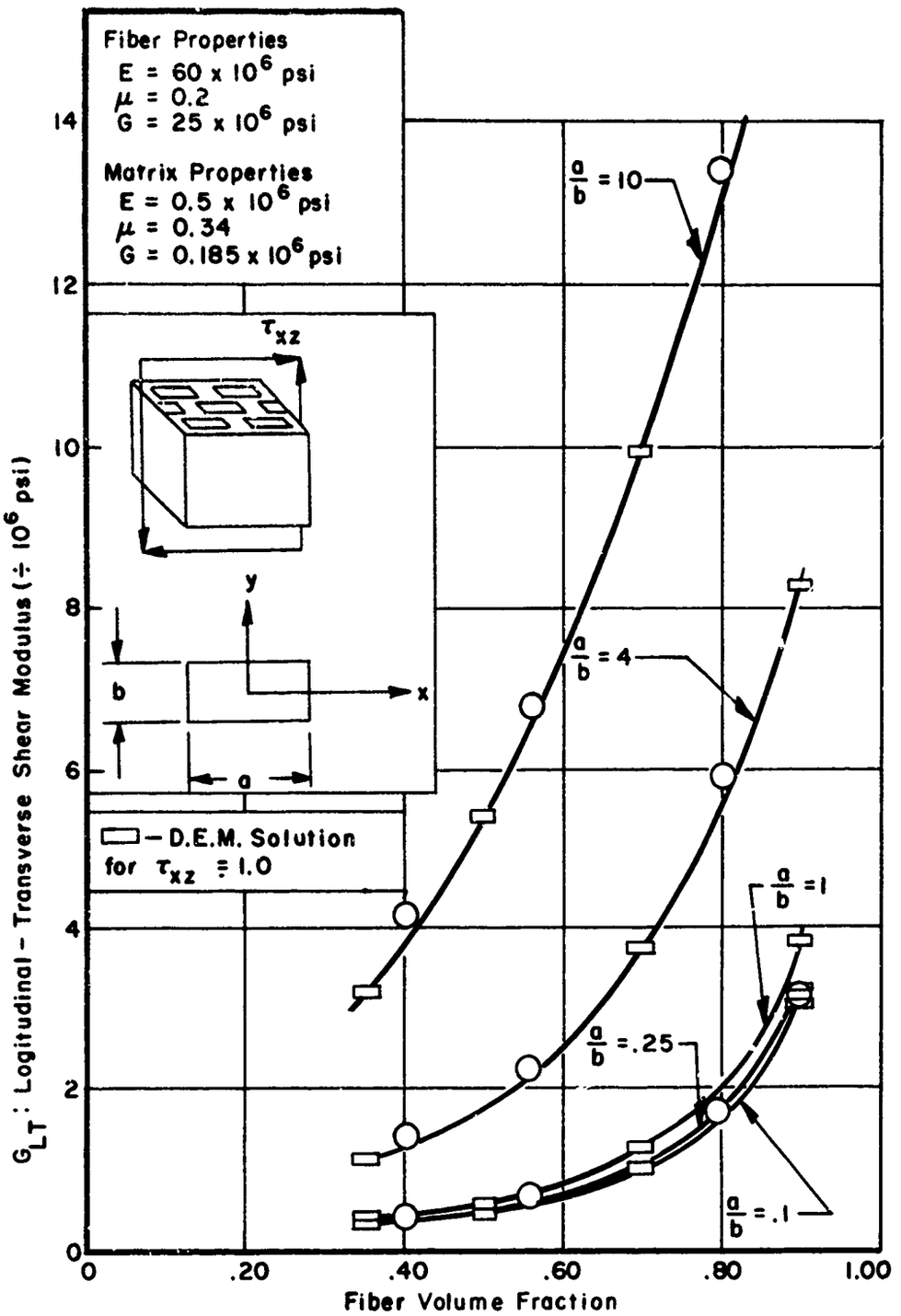

Figure 14. Comparison of Equations 31 and 32 with Finite Element Analysis of Shear Modulus of Composites Containing Rectangularly Shaped Fibers

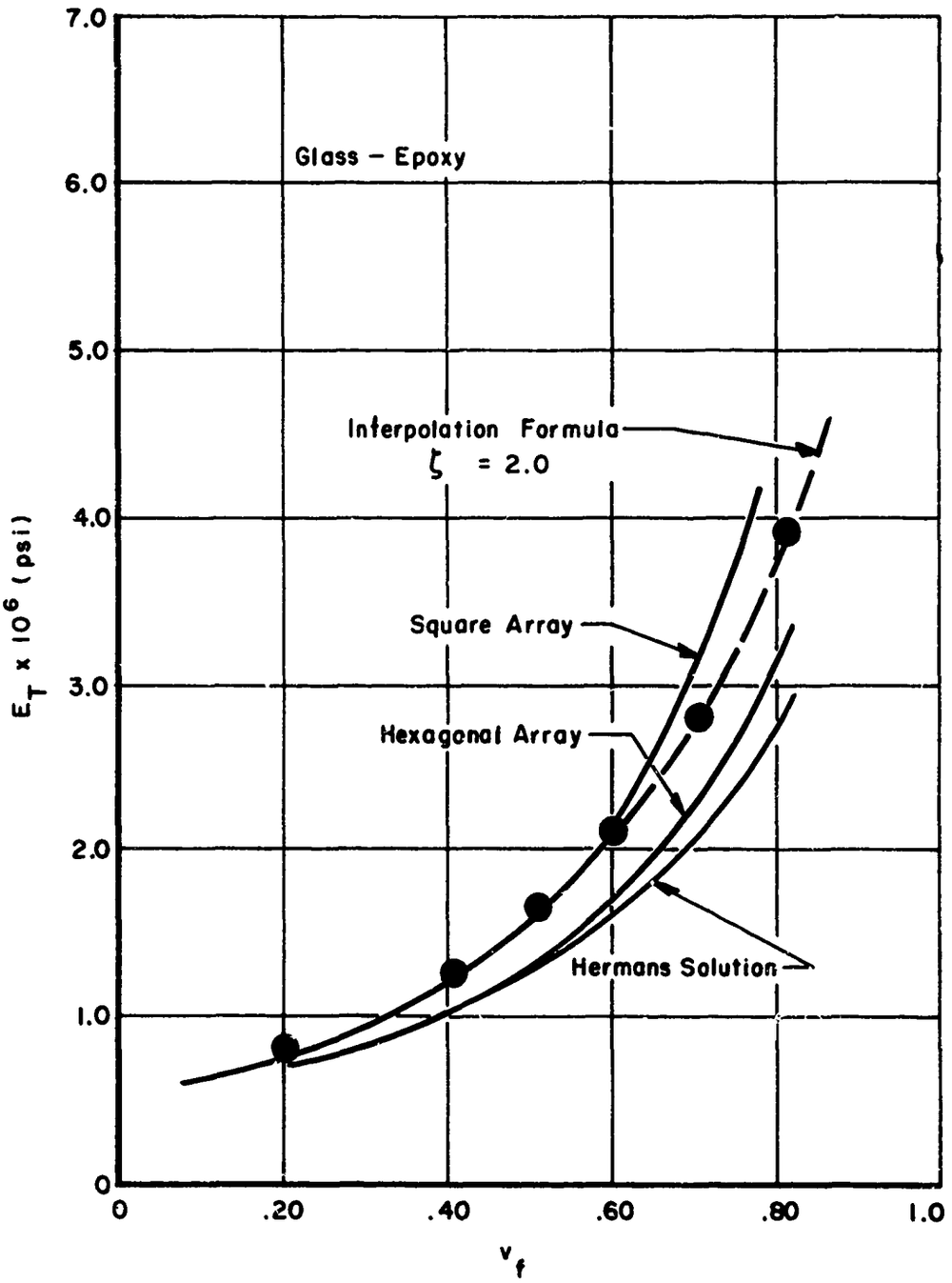

Figure 15. Comparison of Equations 31 and 32 with Results of Finite Element Analysis for Various Packing Geometries of Circular Glass Fibers in an Epoxy Matrix

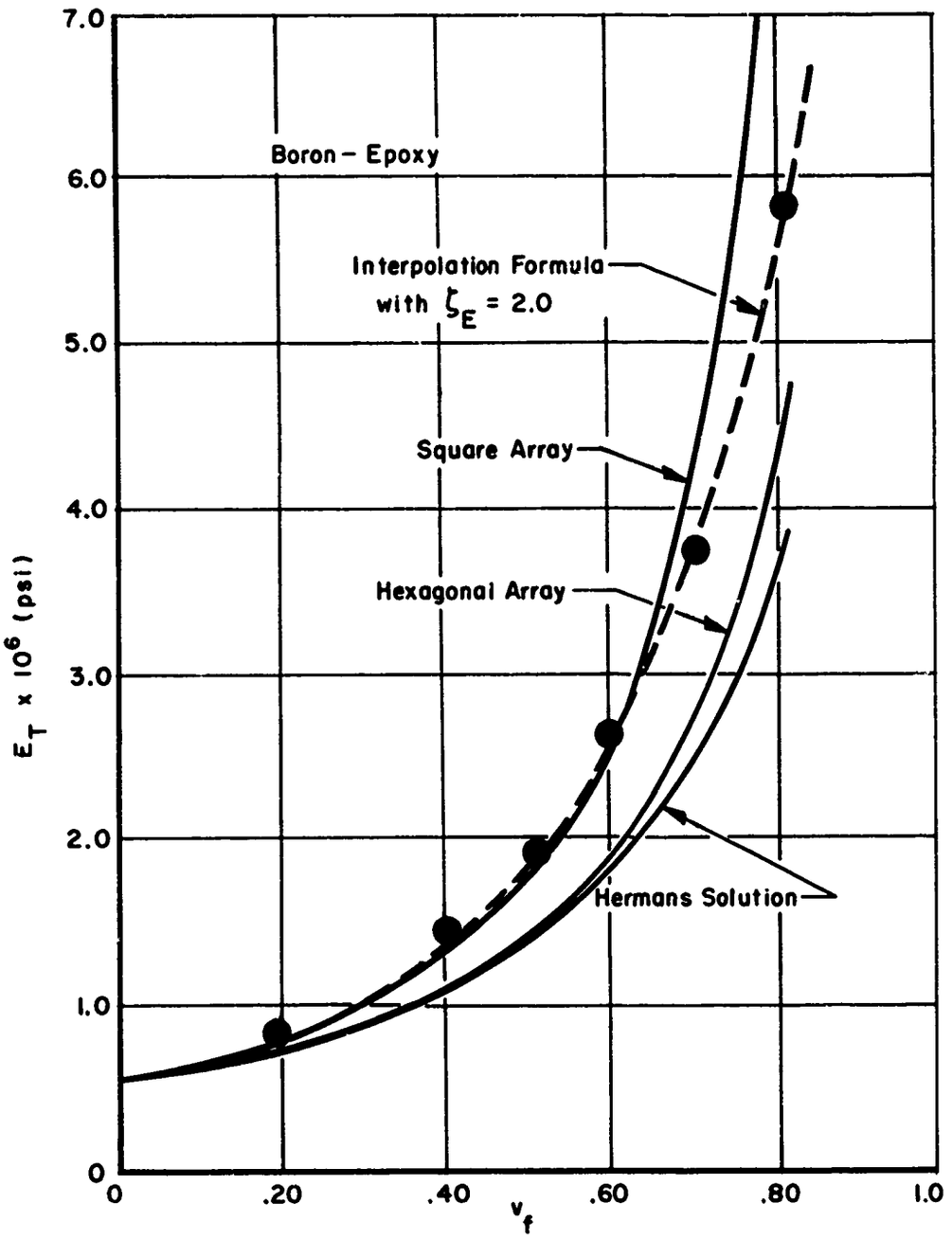

Figure 16. Comparison of Equations 31 and 32 with Results of Finite Element Analysis for Various Packing Geometries of Circular Boron Fibers in an Epoxy Matrix

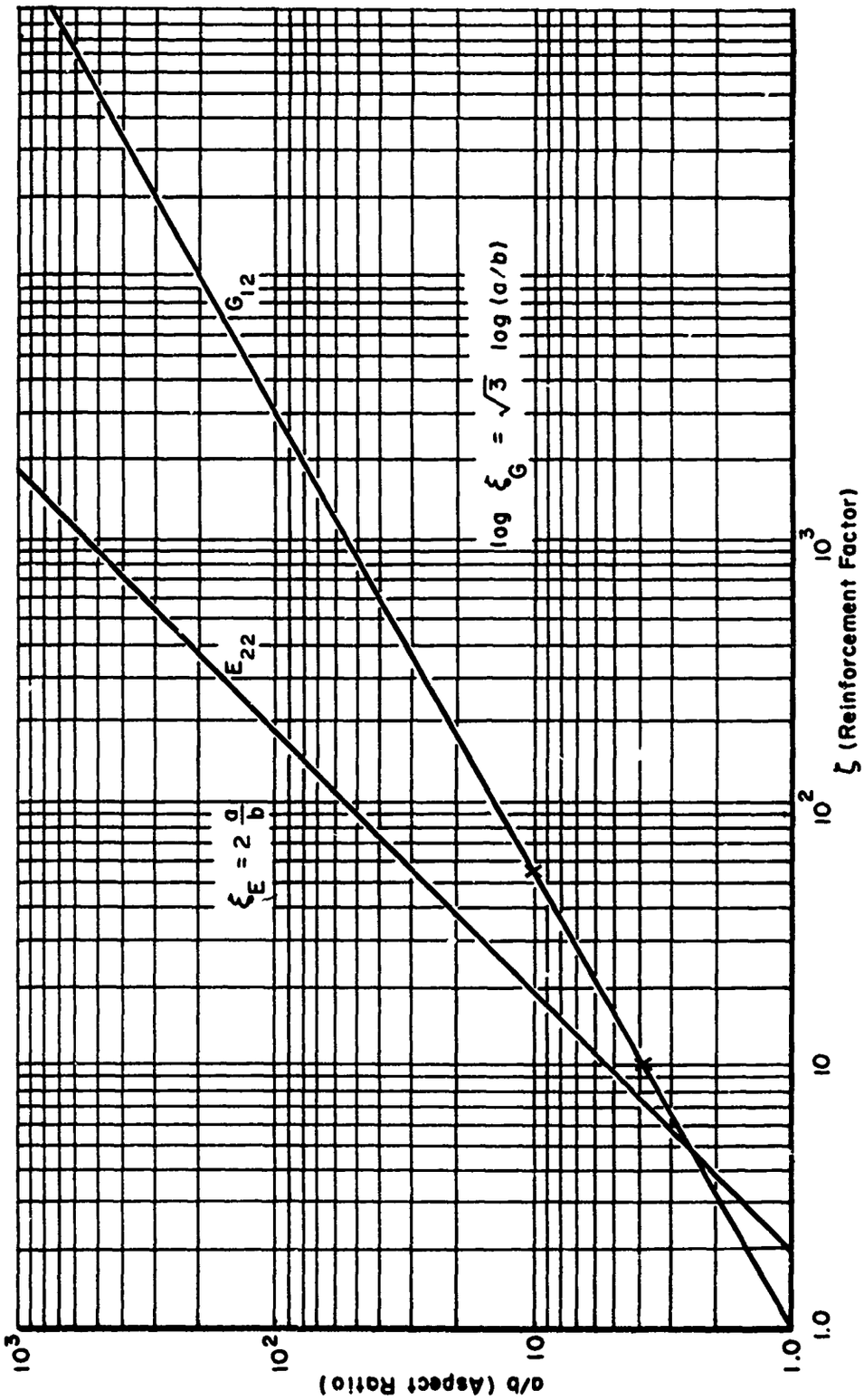

Figure 17. Dependence of Coefficients in Equations 31 and 32 on Aspect Ratio of Rectangularly Shaped Fibers

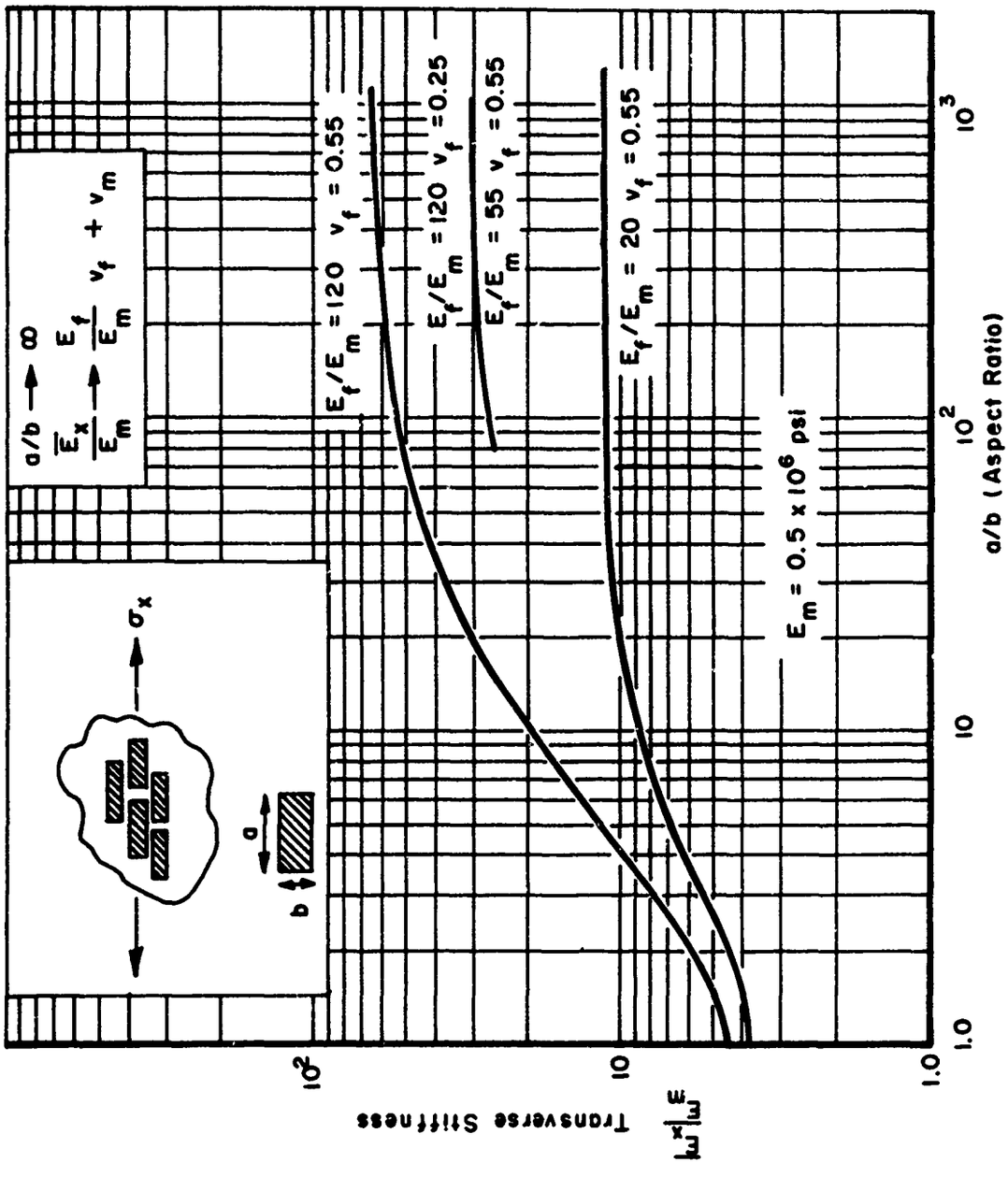

Figure 18. Normalized Prediction of Transverse Modulit of Ribbon Reinforced Composites

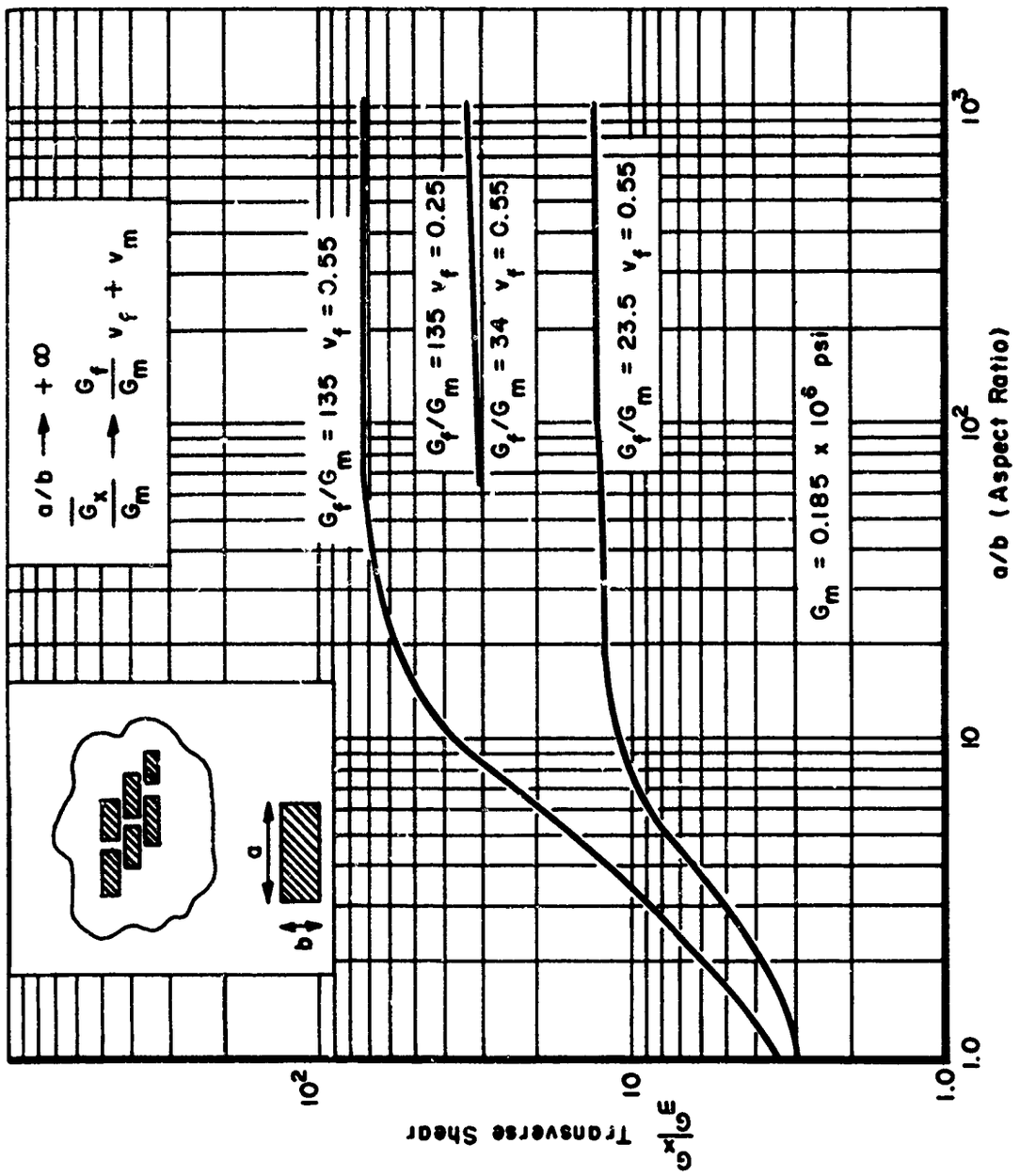

Figure 19. Normalized Prediction of Shear Moduli of Ribbon Reinforced Composites

UNCLASSIFIED

Security Classification

DOCUMENT CONTROL DATA - R & D

(Security classification of title, body of abstract and indexing annotation must be entered when the overall report is classified)

1. ORIGINATING ACTIVITY *(Corporate author)*
Air Force Materials Laboratory
Wright-Patterson Air Force Base, Ohio

2a. REPORT SECURITY CLASSIFICATION
Unclassified

2b. GROUP

3. REPORT TITLE

EFFECTS OF ENVIRONMENTAL FACTORS ON COMPOSITE MATERIALS

4. DESCRIPTIVE NOTES *(Type of report and inclusive dates)*

5. AUTHOR(S) *(First name, middle initial, last name)*

J. C. Halpin

6. REPORT DATE	7a. TOTAL NO. OF PAGES	7b. NO. OF REFS
June 1969	57	23

8a. CONTRACT OR GRANT NO.	9a. ORIGINATOR'S REPORT NUMBER(S)
b. PROJECT NO. 7342	AFML-TR-67-423
c. Task 734202	9b. OTHER REPORT NO(S) *(Any other numbers that may be assigned this report)*
d.	

10. DISTRIBUTION STATEMENT

This document has been approved for public release and sale; its distribution it unlimited. In DDC. Aval frm CFSTI.

11. SUPPLEMENTARY NOTES	12. SPONSORING MILITARY ACTIVITY
	Air Force Materials Laboratory Wright-Patterson Air Force Base, Ohio

13. ABSTRACT

Some of the environmental factors which affect the structural performance of composite materials are discussed. Various possible mechanisms of environmental factors are examined, together with relevant experimental data. Finally, an analytical approach for predicting environmental effects, based on rate theory, is considered.

DD FORM 1 NOV 68 1473

UNCLASSIFIED

Security Classification

14. KEY WORDS	LINK A		LINK B		LINK C	
	ROLE	WT	ROLE	WT	ROLE	WT
Composite Materials						
Micromechanics						
Viscoelasticity						
Fatigue and Fracture						
Environmental Effects						